ARTICLE | Article in Press

Development of flax/kenaf hybrid epoxy composites incorporating sugarcane biochar with enhanced fire performance for potential electrical conduit applications

G. Velmurugan · Jasgurpreet Singh Chohan · S. A. Muhammed Abraar · K. Velusamy · D. Elil Raja · Ramya Maranan · K. Arunprasath · Arun Kumar · Regasa Yadeta Sembeta

Received: 2 September 2026 / Accepted: 9 November 2026
© The Author(s) 2026

Abstract

This study examines the effect of sugarcane biochar on the structural, mechanical, thermal, and fire-related behaviour of flax/kenaf/flax hybrid epoxy composites with different weight contents of biochar (0–6 wt%). FTIR analysis shows that chemical structure changes may occur and that there might be interactions between the biochar and the epoxy matrix. Mechanical characterisation revealed that the measured mechanical properties improved with biochar contents up to 4.5 wt%, but decreased at 6 wt% biochar loading, where changes in filler distribution may have occurred. At 4.5 wt% biochar, the composite exhibited a tensile strength of 38.01 ± 0.55 MPa, flexural strength of 76.12 ± 0.90 MPa, impact strength of 9.62 ± 0.45 kJ/m^2, hardness of 86 ± 1 Shore D, and ILSS of 13.24 ± 0.35 MPa. Additionally, TGA/DTG results revealed that the thermal degradation resistance was enhanced, as the onset degradation temperature rose to 317 °C and the residual char content was 28% at 4.5 wt% biochar. The fire-performance evaluation revealed that the LOI of neat epoxy increased from 19.5 ± 0.5% to 28.4 ± 0.8% at 4.5 wt% biochar. The same formulation showed a lower PHRR of 300.10 ± 9.28 kW/m^2 and THR of 54.03 ± 1.74 MJ/m^2, with delayed ignition and a lower horizontal burning rate. Morphological support for the proposed condensed-phase protective mechanism was obtained from SEM analysis of the post-flammability residues. A cylindrical prototype was fabricated as a proof-of-concept demonstration of the feasibility of forming the composite into a conduit-like geometry, with a length of 300 mm and a wall thickness of 3 mm.

Keywords Natural fibres · Hybrid epoxy composites · Sugarcane biochar · Fire performance · Electrical conduit applications

This Article in Press is shared early to give you faster access to new research. It is citable and carries a permanent DOI. The final edited version will replace it automatically.

https://doi.org/10.1038/s41598-026-80600-3

Published online: 15 November 2026

scientific reports

Introduction

Fiber reinforced plastic (FRP) composites have become increasingly significant in the engineering field due to the possibility of altering their characteristics by choosing the fibres, polymer matrix, fibre architecture, and manufacturing method. FRPs have properties such as low density, high specific strength and stiffness, corrosion resistance, fatigue resistance, and design flexibility, which make them attractive for applications where weight reduction and structural efficiency are important, compared to conventional metallic materials[1]. They are now being applied in several engineering applications, such as the aerospace industry, automotive, marine, wind energy, transportation, sporting goods, and lightweight structural applications. Besides glass- and carbon-fibre-based systems, more research into hybrid- and bio-based composite structures has focused on achieving a combination of mechanical strength, lightweight, low cost, and environmental considerations. Combinations of reinforcement types can yield properties that complement each other, and the overall response of a composite can be tailored for the desired application[2]. Recently, it has been shown that fibre architecture, the characteristics of the interface, laminate configuration, and processing can significantly affect the mechanical and fracture properties of FRP composites[3]. This underscores the need for designing these composite systems, where the reinforcement and matrix are chosen not just to give the required mechanical performance but also to satisfy other application-specific requirements like durability, thermal behaviour, and fire performance[4,5].

The use of synthetic reinforcements in engineering has been a concern, and so the development of natural-fibre-reinforced polymer (NFRP) composites has been encouraged. With their low density, renewable nature, and desirable specific mechanical properties, plant fibres like flax, kenaf, hemp, jute and sisal have received a lot of interest for use in lightweight composite structures[6]. Of these, flax and kenaf are significant bast fibres which have shown substantial potential as polymer reinforcement. Flax fibres have been well studied within thermoset and thermoplastic matrices, as the architecture of the fibre, its direction, fibre content, surface treatment, matrix, and processing conditions all have a significant effect on the performance of the fibre composite[7]. Low density, fast growth, and good mechanical properties are also the reasons why kenaf fibres have been studied as polymer reinforcement. But, because of their hydrophilic nature, the moisture sensitivity of both fibres and the limited compatibility of fibres with relatively hydrophobic polymer matrices can influence fibre–matrix adhesion and stress transfer. Hence, it is common practice to modify the surface and adopt the proper composite architecture for better interfacial interactions and composite performance. Hybridization of different natural fibres can be seen as a tool to combine complementary characteristics in a single laminate in this context[8]. Specifically, earlier studies[9] on kenaf/flax–epoxy hybrid composites have shown that mechanical properties such as tensile, flexural, interlaminar shear, fracture and moisture-related properties are dependent on the type of fibres and stacking sequence, and hence fibre architecture plays a significant role in determining the behaviour of the hybrid natural fibre–epoxy composites.

Natural fibre composites have mechanical and lightweight benefits, but thermal degradation and combustion are significant drawbacks where fire performance is critical[10,11]. Major components of lignocellulosic fibres are cellulose, hemicellulose, and lignin, which can produce combustible volatile products which can produce combustible volatile products and undergo thermal decomposition at elevated temperature. The fire behaviour of a composite made with the addition of a polymeric phase (epoxy) depends on the characteristics of the thermal degradation of the matrix, the type of fibre, the fibre content, the fibre architecture, and the interactions between the fibre and the polymeric phase. Furthermore, the amount of condensed-phase residue formed and its stability during combustion may affect the heat and mass transfer across the material and thus the ignition behavior, heat release, and burning rate[10,12]. The flammability and thermal stability of the natural-fibre-reinforced polymer composites have been identified as important challenges that need to be overcome if they are to be used in engineering applications with enhanced fire properties. Several methods have been explored, such as fibre treatment, modifying the matrix, coatings on the surface, mineral and phosphorus-containing additives, and carbonaceous

fillers. However, the challenge of materials design for achieving a better fire performance while maintaining the mechanical properties of natural-fibre-reinforced epoxy composites is a formidable one[12,13].

This growing interest in biochar as the carbonaceous filler in polymer composites is attributed to its tailorable physicochemical properties from biomass feedstock and thermochemical processing conditions[14]. Relatively high carbon content, aromatic structure, thermal stability, and surface functionality may influence the thermal degradation, mechanical and fire behavior of polymeric materials[15,16]. A condensed-phase barrier is formed by thermally stable carbonaceous residues in polymer composite materials exposed to fire, which may prevent heat and mass transfer between the burning composite and the environment, and consequently, reduce the heat release and retard the degradation. Previous work has shown that biochar incorporation could enhance the thermal stability and reduce the peak heat-release rate of polymer-based systems, but the effects may vary significantly with the characteristics of the biochar, loadings, dispersion, and compatibility with the polymer matrix[16,17]. Carbonaceous fillers are thus being considered as one means to overcome the natural-fibre-reinforced polymers' fire performance drawbacks while maintaining their structural properties. Recent reviews have focused on the interactions between polymer matrix, natural fibres, and the flame retardant/carbonaceous additives, as well as the need to improve fire performance in conjunction with mechanical performance and structural integrity[17,18]. But biochar may not exhibit the same behaviour at all loadings; high loadings can have a negative impact on dispersion, processing, interfacial interactions, and mechanical properties. Hence, it is crucial to find an adequate biochar loading for a balance between mechanical and fire-related properties[16,18].

Recent research has also shown that carbonaceous materials derived from biomass, as well as biochar-based fillers, are suitable for the production of multi-functional polymer composites[16]. Biochar and other carbon structures derived from biomass can enhance mechanical reinforcement as well as thermal management and functional properties depending on their structure, surface chemistry, particle morphology and interactions with the surrounding matrix. For instance, Ren et al.[19] prepared all-biomass-derived nanocomposite films composed of carbon quantum dots and carbon nanosheets from cellulose nanofibres, and characterized mechanical, thermal and degradation properties, suggesting that the biomass-derived carbon structures could be used as functional components in composite materials. Recently, Ren et al.[20] reported the fabrication of all-biomass nanocomposite films using cellulose nanofibres and carbon spheres derived from pyrolysis, which led to ordered carbon nanostructures that enhanced the interfacial interaction, thermal conductivity, mechanical properties and electromagnetic-interference shielding properties. More recently, Yu et al.[21] have shown that biochar could be used as a component of a synergistic network involving polypyrrole and the polymer matrix to impart mechanical robustness and multifunctional electromagnetic and sensing properties. These studies illustrate the more general possibilities of biomass-derived carbonaceous materials to alter the structure and functional behaviour of polymer-based systems. The materials reported, though, are cellulose-derived nanostructures, carbon spheres or biochar-containing hydrogel systems, not waste-derived sugarcane biochar incorporated into a woven flax/kenaf/flax epoxy laminate. Furthermore, their focus is on multifunctional properties like degradation, thermal management, electromagnetic shielding or sensing, instead of the simultaneous evaluation of mechanical and fire properties in a hybrid natural-fibre epoxy architecture. This distinction emphasises the need to explore the effect of sugarcane biochar specifically in hybrid flax/kenaf epoxy composites. Table 1 reveals the representative studies of biochar- or biomass-based carbon-containing polymer composites, showing their polymer matrix types, properties studied, and the particular research gaps that are pertinent to the current study.

While biochar and other carbon-based fillers have been shown to influence the mechanical, thermal and fire properties of polymer composites, the reported systems can be significantly different with regard to matrix type, reinforcement structure, origin of the filler and properties to be targeted. The majority of the literature has been directed towards thermoplastic matrices, single natural fibre composites, chemically modified flame retarded systems or multifunctional composites based on biochar for primary functions like thermal management, electromagnetic interference shielding, and sensing. This creates a research gap that remains to be addressed in terms of how the waste-derived sugarcane biochar interacts with the woven flax/kenaf/flax architecture within the epoxy matrix and how the loading affects mechanical and fire-performance properties in tandem. In particular, the effect

Table 1 Comparative summary of reported biochar- and biomass-derived carbon-containing polymer composites, their investigated properties, key findings, and relevance to the present study.

Author (Year)	Composite system	Biochar / carbonaceous material	Main investigation	Key findings relevant to the present study	Distinction from present study	References
Zuccarello et al. (2021)	Agave sisalana fibre/epoxy biocomposite	Biochar	Mechanical performance, interfacial behaviour and durability	Biochar incorporation affected the matrix/fibre interphase and improved static tensile performance and fatigue life at an intermediate loading	Short Agave-fibre epoxy system; did not investigate woven flax/kenaf hybrid architecture or fire performance	22
Kishore et al. (2022)	Areca-fibre/epoxy composite	Papaya-slice biochar	Mechanical, thermal-conductivity and dielectric properties	Biochar/fibre incorporation improved tensile, flexural and impact properties and modified thermal and dielectric behaviour	Chopped areca fibre and papaya biochar; focus was not on fire performance or flax/kenaf hybrid laminates	23
Malik et al. (2023)	Kenaf/flax hybrid epoxy composites	—	Physical and mechanical properties, stacking sequence and moisture behaviour	Demonstrated that fibre type and stacking sequence influence mechanical and moisture-related performance of kenaf/flax hybrid epoxy laminates	Does not incorporate biochar; fire performance was not the principal focus	9
Kumar et al. (2024)	Curtain-climber-fibre/epoxy biocomposite	*Kigelia pinnata* biochar	Mechanical, thermal and dielectric properties	Incorporation of 5 wt% biochar with fibre reinforcement enhanced the measured composite properties	Different natural fibre and biochar feedstock; no flax/kenaf/flax architecture or fire-performance investigation	24
Bifulco et al. (2024)	Modified epoxy nanocomposite	Coffee-waste-derived biochar	Thermal, fire and mechanical behaviour	Biochar contributed to reduced PHRR and acted in the condensed phase; stronger flame-retardant performance was obtained in combination with other flame-retardant components	Epoxy nanocomposite without natural-fibre laminate reinforcement; used coffee biochar and additional flame-retardant components	25
Sahoo & Dash (2025)	Jute/coir and jute/coir hybrid epoxy composites	Coconut-shell biochar	Mechanical, thermal, water absorption, morphology and statistical analysis	Investigated biochar-containing natural-fibre and hybrid epoxy systems using mechanical, thermal, water-absorption and morphological characterization	Used jute/coir rather than flax/kenaf/flax and coconut-shell rather than sugarcane biochar; fire performance was not the primary focus	26
Ren et al. (2025)	All-biomass nanocomposite films	Carbon quantum dots/carbon nanosheets derived from cellulose	Mechanical, thermal and degradation behaviour	Biomass-derived carbon structures provided multifunctional mechanical and thermal properties	Nanocomposite film based on cellulose-derived carbon structures, rather than biochar-filled natural-fibre/epoxy laminates	19
Ren et al. (2025)	All-biomass nanocomposite films	Pyrolysis-derived carbon spheres	Thermal management and EMI shielding	Pyrolysis-derived carbon structures contributed to interfacial interactions, thermal conductivity and EMI shielding	Focused on all-biomass nanocomposite films and functional properties rather than fire behaviour of fibre/epoxy laminates	20
Yu et al. (2026)	Sodium alginate/polyacrylamide multifunctional hydrogel	Biochar with polypyrrole	Mechanical robustness, EMI shielding and strain sensing	Biochar participated in a synergistic network that contributed to mechanical and multifunctional behaviour	Hydrogel system with polypyrrole; fundamentally different matrix and application from the present fibre/epoxy composite	21
Present study	Flax/kenaf/flax hybrid epoxy composite	Sugarcane-waste-derived biochar	Mechanical, microstructural, thermal and fire performance	Systematic investigation of biochar incorporation at 0–6 wt% and evaluation of its influence on composite performance; conduit-like prototype fabricated	Combines woven flax/kenaf/flax hybrid architecture with sugarcane-waste-derived biochar and evaluates mechanical and fire-related performance within the same composite system	

of biochar loading, on mechanical response, thermal degradation, char-residue development and fire behaviour are poorly understood in this specific hybrid laminate. This is essential because increasing the performance of fire resistance in natural fibre/epoxy composites should not result in any loss of mechanical functionality. Thus, the present study explores the physical and chemical characteristics of biochar made from sugarcane wastes (SCW) at varying nominal loadings to a hybrid epoxy composite (flax/kenaf/flax). The study focuses on determining the composition-dependent changes in the mechanical, microstructural, thermal and fire-performance properties. The study also investigates the ability of the composite to be formed into a conduit-like geometry by the fabrication of a proof-of-concept prototype for electrical conduit applications.

Experimental works

Materials

Go Green products at Valasaravakkam, Chennai, Tamil Nadu, India, provided woven flax (1.40 g/cm^3) and kenaf fabric (1.20 g/cm^3) with 250 GSM for the composite fabrication process. Furthermore, HY 951 hardener (density 0.97 g/cm^3, flash point 110ºC) and LY 556 type epoxy resin (density 1.15 g/cm^3, flash point 200ºC) were bought from GVR Enterprises in Madurai, Tamil Nadu, India. The raw material for pyrolysis to create biochar was sugarcane husks, which were purchased from nearby commercial juice stores in Tirupati, Andhra Pradesh, India. The same GVR Enterprises provided NaOH pellets with a density of 2.13 g/cm^3 (solid) and a molecular weight of 40 g/mol. Figure 1 shows the matrix and reinforcement materials.

NaOH Pretreatment

The flax and kenaf fiber mats were cleaned first under running water to remove any unwanted materials adhering to the surface of the mats. After that, the fibers were sun-dried for around 24 h to allow the moisture to evaporate. For approximately four hours, the cleaned fibers were steeped in a 5 wt% NaOH solution at a ratio of 20:1 mL/g. After that, the fibers were washed with double-distilled water to remove any residual NaOH solutions. The fibers were then neutralized with a diluted form of acetic acid and dried for around 48 h to achieve a consistent weight[27]. Figure 2 shows the photographic image of NaOH treatment of natural fibers.

Figure 3 clearly explains the structural representation of natural fiber before and after NaOH treatment. The chemical reaction of the NaOH treatment is explained by Eq. (1) [28].



Fig. 1 Photographic images of (**a**) Flax fiber; (**b**) Kenaf fiber and (**c**) Matrix materials

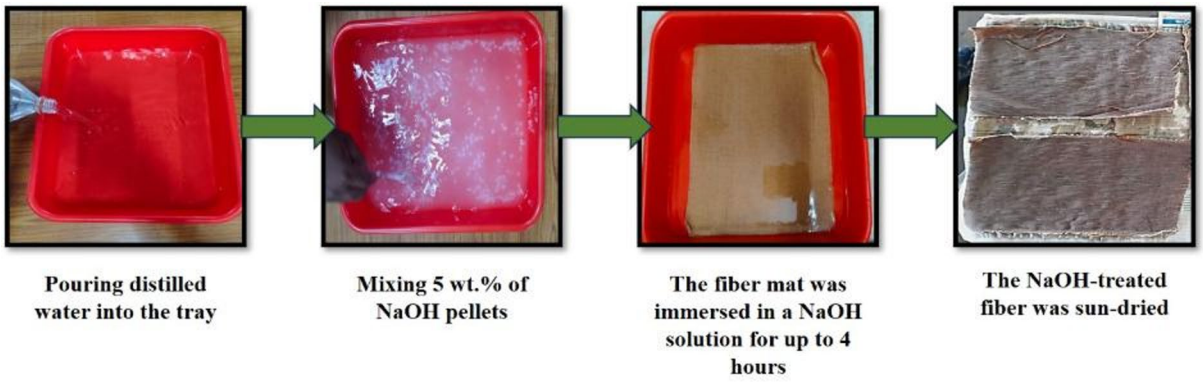


Fig. 2 Photographic images of NaOH treatment of natural flax and kenaf fibers.



Fig. 3 Structural representation of natural fibers before and after NaOH treatment.

$$Fiber - OH + NaOH \rightarrow Fiber - O^{-}Na^{+} + H_2O \quad (1)$$

This process is expected to remove hemicellulose, lignin, and surface impurities and modify the fibre surface.

Biochar preparation

The sugarcane husks were collected and cleaned to remove dirt and surface contaminants by flushing them with ample water. Washed husks were air-dried in the sun for 24 h and then oven-dried at 70 °C for 10 h to completely dry the husks. The dried sugarcane husks were then slowly pyrolysed in a furnace using a steel container under oxygen limited conditions. The material was heated up to the maximum temperature of 650 °C with a heating rate of about 10 °C/min and kept at 650 °C for about 1 h[29]. Once the pyrolysis treatment was completed, the furnace was allowed to cool before the biochar was collected, so that the hot char did not have to come in direct contact with the atmosphere. The resulting biochar was then ground in a Ball-Milling machine and a particle size of about 30–50 µm was obtained by sieve analysis. The prepared biochar was collected and stored under dry conditions for further use in the composite fabrication[30]. The overall biochar preparation process is shown in Fig. 4.

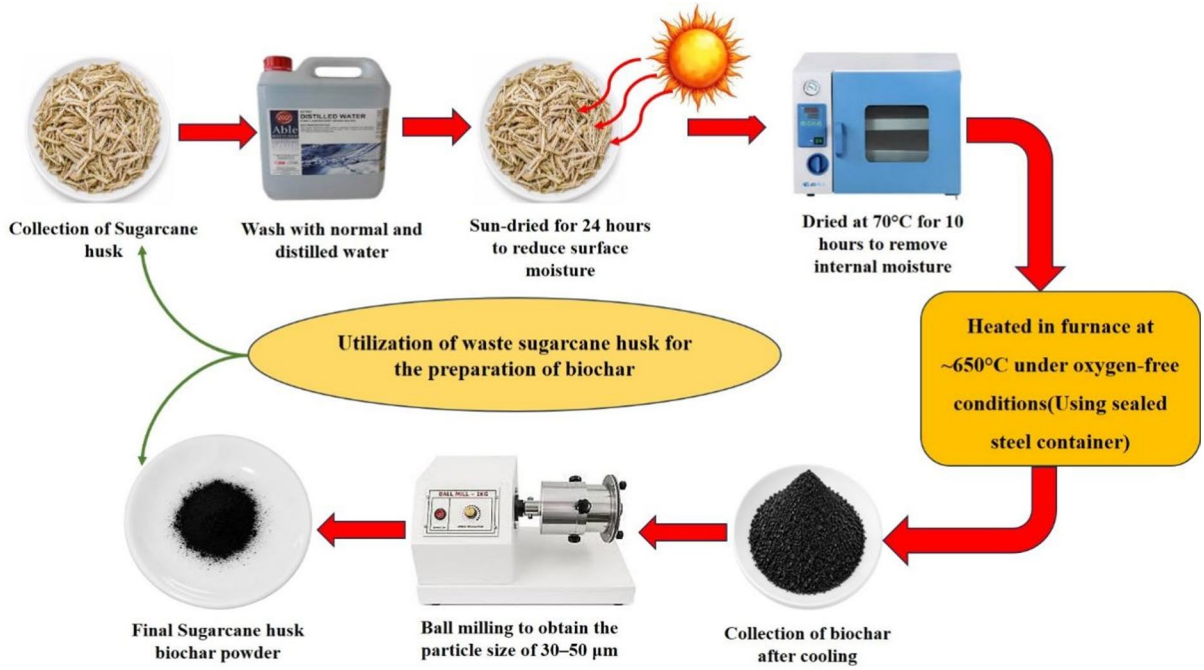


Fig. 4 Step by step process of biochar preparation from waste-based sugarcane husk

Composite fabrication

Fabrication of the composites was done using a mixture of manual hand lay-up and compression molding. The two woven fabrics (flax and kenaf) with an areal density of 250 g/m^2 were stacked in a predefined stacking sequence of flax/kenaf/flax in a cast iron mold of 300 × 300 × 3 mm^3. The plain epoxy matrix was made of LY 556 epoxy resin and HY 951 hardener at a 10:1 ratio, resulting in a total matrix mass of 297.28 g for Sample A (plain epoxy). The total dry fibre mass for the flax/kenaf/flax hybrid laminate was 67.50 g, of which 45.00 g was the flax fibre and 22.50 g was the kenaf fibre. Sample B had a combined fibre-matrix mass of 364.78 g, which represents 18.50 wt% fibre and 81.50 wt% epoxy matrix. The fibre content was kept under 20 wt. % to ensure sufficient availability of matrix for fibre impregnation and fibre–matrix interaction, as previous reports indicated that mechanical properties of natural-fibre/epoxy composites are significantly influenced by fibre content and fibre–matrix interaction. Sugarcane biochar was incorporated at nominal loadings of 0, 1.5, 3, 4.5, and 6 wt% (0, 4.46, 8.92, 13.38, and 17.84 g, respectively) relative to the total epoxy matrix mass. The required amount of biochar was dispersed into the epoxy resin with a probe sonicator that ran at a frequency of about 20 kHz for 35 min, prior to the addition of the hardener. The biochar filled resin was then used to impregnate the fibre mats during the hand lay-up process to ensure uniform impregnation. After lay-up, the laminate was compressed at 110 °C and 5 MPa for 40 min to promote consolidation and minimize the formation of voids[24,31,32]. Molded laminates were cooled under pressure and then cured at room temperature for 24 h before processing and testing. Different composite formulations and their composition are shown in Table 2 and the fabrication process and prepared test specimens are shown in Fig. 5.

Table 2 Configurations of fabricated composite with biochar content.

Sl. No	Symbol	Combination	Biochar weight proportion (wt%)
1	A	Plain Epoxy	0
2	B	Flax/Kenaf/Flax	0
3	C	Flax/Kenaf/Flax	1.5
4	D	Flax/Kenaf/Flax	3
5	E	Flax/Kenaf/Flax	4.5
6	F	Flax/Kenaf/Flax	6



Fig. 5 Sequential fabrication process of flax/kenaf/sugarcane biochar-based hybrid composites and preparation of mechanical test specimens

Material characterization

Structural analysis

An X-ray diffractometer with Cu Kα was used to analyze the structural characteristics of the prepared sugarcane biochar. The XRD analysis was conducted with 45 kV and 40 mA, and a wavelength of 1.54 Å, with the diffraction pattern recorded from 5°–100° (2θ), to assess the structural characteristics of the biochar. The elemental composition of the prepared sugarcane biochar was analyzed by energy-dispersive X-ray spectroscopy (EDX) at an accelerating voltage of 15.0 kV, which showed the main elements present in the biochar. Fourier Transform Infrared Spectroscopy (FTIR) analyses was conducted on the prepared biochar and biochar containing hybrid composites in the wavenumber range of 4000–400 cm^{-1} at a resolution of 4 cm^{-1} using a Jasco FTIR 6600 spectrometer, Japan to find the functional groups present in them. Samples were prepared by the KBr pellet method with the ratio of sample to KBr as 1:100 and analyzed on the FTIR spectrometer. The FTIR measurements were carried out at Sathyabama Institute of Science and Technology, Chennai, Tamil Nadu, India.

Thermal analysis (TGA/DTG)

Thermogravimetric analysis (TGA) and derivative thermogravimetric (DTG) analysis was carried out using a Netzsch STA 2500 Regulus thermal analyzer at SRM Institute of Science and Technology, Chennai, Tamil Nadu, India. The samples were tested for their thermal degradation behaviour in nitrogen at 10 °C/min and under a controlled flow rate of 40–60 mL/min with a temperature range of 30–800 °C. All samples were tested under the same experimental conditions to allow comparison of the thermal degradation behaviour of the samples. The TGA and DTG curves were obtained to determine the onset degradation temperature, main stages of degradation and residual mass/char yield for the samples.

Mechanical characterization

The tensile properties of woven flax/kenaf/flax hybrid composite laminates were tested on Instron universal testing machine with a 10 kN load capacity, as per ASTM D3039. The load–displacement response was obtained by testing the prepared specimens at a constant crosshead speed of 2.5 mm/min and the tensile strength, tensile modulus, and elongation at break were obtained from the stress–strain response. The flexural properties of the hybrid composite laminates were determined by the three-point bending test specified in ASTM D790-10, with the dimension of the specimen being $60 \times 12.7 \times 3$ mm^3, the support span was 50 mm, and the crosshead speed was 2.5 mm/min. Izod impact strength was measured according to ASTM D256 with the dimensions of the specimen being $64 \times 12.7 \times 3$ mm^3. Hardness of the developed composites was determined by Shore D durometer as per ASTM D2240 with test pieces having the dimensions $50 \times 50 \times 3$ mm^3. Interlaminar shear strength (ILSS) of the flax/kenaf/flax laminated composites was measured by short beam shear method based on ASTM D2344. Approximately $18 \times 6 \times 3$ mm^3 specimens were prepared with a length-to-thickness ratio of 6:1 and a width-to-thickness ratio of 2:1. A support span-to-thickness ratio of 4:1 was used, corresponding to a support span of approximately 12 mm.

The mechanical tests were performed at room temperature. The mechanical data are presented as mean ± SD, n = 3 specimens were tested for each mechanical property. The standard deviation (SD) of the repeated measurements was calculated and reported in the mechanical-property tables and figures. The differences among the composite formulations were statistically analyzed using one-way analysis of variance (ANOVA) at a 5% significant level. Scanning electron microscopy (SEM) was used to examine the mechanisms of fibre/matrix bonding, characteristics of matrix fracture, presence of voids, filler distribution and the morphology of the composites.

Fire retardant characteristics

The fire performance of the fabricated composite specimens was evaluated usig limiting oxygen index (LOI), cone calorimetry and horizontal burning test. Specimens of size 125×13x3 mm^3 were tested in the horizontal burning test as per ASTM D635-03. A horizontal-burning test was used to determine the burning time and burning rate; the burning rate was calculated from the burning distance measured and the corresponding burning time. The horizontal burning characteristics were tested as per ASTM D635-03. Cone calorimetry tests were performed to conform to ASTM E1354-17 with dimensions of specimens of $100 \times 100 \times 3$ mm^3. The composite specimens were tested for reaction to fire with an external heat flux of 50 kW/m2. Parameters measured were time to ignition (TTI), time to peak heat release rate (TPHRR), peak heat release rate (PHRR) and total heat release (THR). The experimental setup for the limiting oxygen index (LOI) and cone calorimeter tests of prepared composite materials is illustrated in (a) and (b), respectively, of Fig. 6.

The specimens used for the limiting oxygen index test (LOI) were rectangular in shape, with dimensions of $100 \times 6.5 \times 3$ mm^3, and were tested according to ASTM D2863-17. The oxygen index tester from Sataton Limited was used for the measurements of LOI. All the fire characterization experiments were performed at CIPET, Chennai, Tamil Nadu, India. Each fire-performance measurement was replicated three times, and reported as the

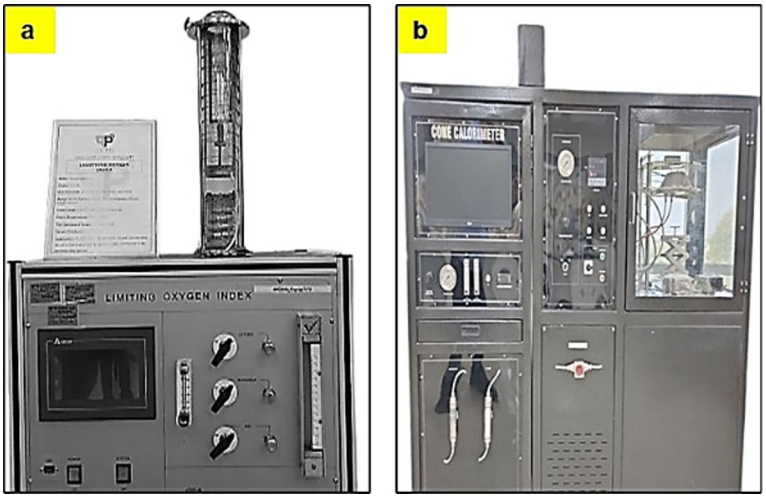


Fig. 6 Photographic images of (**a**) limiting oxygen index test and (**b**) cone calorimeter apparatus.

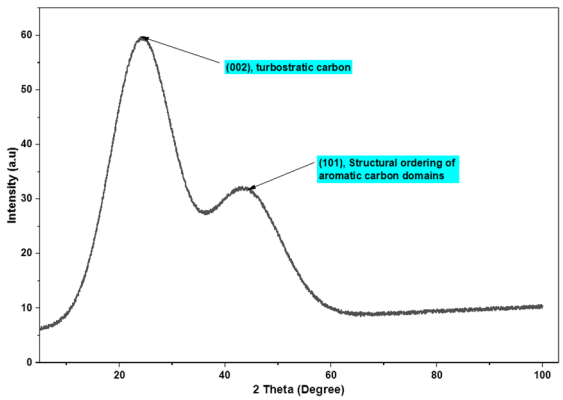


Fig. 7 XRD analysis of prepared sugarcane biochar

mean ± standard deviation (SD). For each composite formulation, the test conditions and specimen dimensions were kept the same so as to facilitate the comparison of their fire-performance characteristics.

Result and discussion

Structural analysis of hybrid composites

X-ray diffraction analysis of sugarcane biochar

The X-ray diffraction (XRD) pattern of the prepared sugarcane biochar is shown in Fig. 7. A broad, relatively diffuse diffraction peak is present at about $2\theta = 24.45°$ with a weaker broad peak between $2\theta = 42–44°$. The first reflection can be attributed to the (002) plane associated with the stacking of disordered carbon layers, while the broad reflection near 43.8° can be associated with in-plane ordering of carbon domains corresponding to the (100) plane[33]. The wide range of both features suggests that there is a low level of long-range structural ordering relative to highly-crystalline graphite. The d-spacing values corresponding to the observed maxima at about 24.45° and 43.8° were calculated as approximately 3.64 Å and 2.06 Å respectively using a Cu Kα radiation wavelength ($\lambda = 1.54$ Å).

The wide diffraction profile is related to the structural change of the lignocellulosic components of the sugarcane husk during pyrolysis. Thermal decomposition of cellulose, hemicellulose and lignin leads to the increased

presence of aromatic, carbon-rich domains, but also to a high structural disorder. As a result, the biochar produced has properties of turbostratic or poorly ordered carbon and not highly crystalline graphite[34,35]. The lack of narrow and intense graphitic reflections is further evidence of the presence of randomly oriented and structurally imperfect carbon layers.

Thus, the XRD profile can be used to confirm the formation of a carbonaceous structure that is predominantly disordered in the prepared sugarcane biochar. This structural information is used as a basis for interpreting the role of the biochar as a carbonaceous filler in the hybrid epoxy composite; the effects on mechanical performance, thermal performance and fire performance are discussed separately in the respective sections.

EDX analysis of sugarcane-husk biochar

Energy-dispersive X-ray spectroscopy (EDX) was used to determine the elemental composition of sugarcane-husk biochar and the EDX spectrum and elemental composition are shown in Fig. 8. Carbon was the predominant detected element, accounting for 91.46 wt% (95.22 at%), followed by oxygen at 3.96 wt% (3.10 at%). Minor elements, including Ca (1.83 wt%), Si (1.22 wt%), K (0.91 wt%), Mg (0.41 wt%), and Cl (0.20 wt%), were also detected. The high relative carbon content confirms the carbon – rich nature of the prepared sugarcane-husk biochar, and the presence of minor inorganic elements may be due to mineral components that were not volatilized during the thermal conversion process[36]. The EDX results give additional elemental information to the FTIR analysis that describes the functional groups in the biochar. The elemental percentages measured by EDX are semiquantitative and cannot be taken as representative of bulk elemental composition because EDX is a micro area surface analysis method[37].

FTIR analysis

FTIR spectra of the developed composites were recorded from 4000 to 400 cm^{-1} to understand the functional group regions corresponding to the epoxy matrix, natural fibres treated with alkali and sugarcane-husk biochar. The spectra of Samples A–F are shown in Fig. 9. The FTIR spectra of the alkali-treated flax, alkali-treated kenaf, and sugarcane-husk biochar were also studied as reference materials for the interpretation of the composite spectra.

The spectrum of Sample A (plain LY556/HY951 epoxy matrix) shows the characteristic absorption bands at ~3426, ~2920, ~1604, ~1510, ~1238, ~1070, ~916 and ~832 cm^{-1}. The bands around 1604 and 1510 cm^{-1} are linked to the aromatic skeletal vibrations of the epoxy matrix, while the band around 2920 cm^{-1} is linked to aliphatic C–H stretching. The bands at 1238 and 1070 cm^{-1} are related to C–O-containing structures, and the band at 832 cm^{-1} is consistent with the vibrations that involve C–H of the aromatic system in the bisphenol-A-based

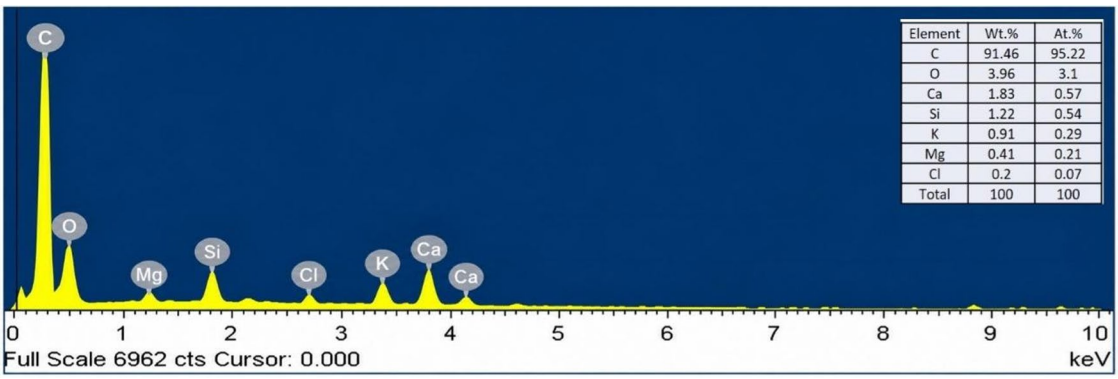


Fig. 8 EDX spectrum and elemental composition of sugarcane-husk biochar.

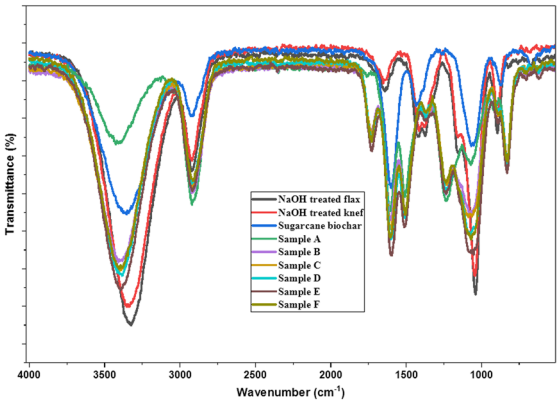


Fig. 9 FTIR spectra of plain epoxy, alkali-treated flax and kenaf fibres, sugarcane-husk biochar, and flax/kenaf/flax hybrid epoxy composites containing different concentrations of biochar.

epoxy system. The areas of the neat epoxy spectrum around ~ 1600 cm^{-1} and ~ 830 cm^{-1} are of particular importance as they cannot be used later as unique signatures of the incorporated biochar.

The alkali-treated flax and kenaf fibres show characteristic absorption features of lignocellulosic fibres. Alkali-treated flax exhibits prominent bands at approximately 3324, 2922, 1640, 1422, 1040, and 894 cm^{-1}, whereas alkali-treated kenaf shows corresponding features at approximately 3334, 2920, 1652, 1416, 1044, and 894 cm^{-1}. The wide absorption band around 3324–3334 cm^{-1} is related to O–H stretching of hydroxyl containing components, and the bands around 2920 cm^{-1} are related to aliphatic C–H stretching. The absorption at 1040–1044 cm^{-1} is related to absorption of C–O compositions of the lignocellulosic components. There have been reports on similar O–H, C–H, carbonyl and C–O related regions for natural fibres and kenaf based system[38].

The sugarcane-husk biochar exhibits characteristic bands at approximately 3354, 2914, 1600, 1434, 1068, 876, and 662 cm^{-1}. Recent characterization of sugarcane-derived extracts has also demonstrated the presence of phenolic and other oxygen-containing constituents, highlighting the chemical complexity of sugarcane-derived materials[39]. However, the chemical composition of the present biochar is expected to differ because of the pyrolysis treatment. The broad band at 3354 cm^{-1} can be attributed to the presence of residual hydroxyl groups on the surface, whereas the band at 2914 cm^{-1} can be assigned to aliphatic C–H stretching. The bands around 1600 cm^{-1} are related to aromatic/conjugated carbon structures, and the bands near 1434 cm^{-1} and 1068 cm^{-1} are related to C–H deformation and C–O-containing structures, respectively. The lower-wavenumber bands (~ 876 and ~ 662 cm^{-1}) are consistent with vibrations of aromatic or oxygen-containing surface structures. A similar FTIR region has been reported in biochars derived from sugarcane, where the O–H stretching band is within the region of 3600–3200 cm^{-1}, aliphatic C–H are in the region of about 2920 cm^{-1}, aromatic or conjugated structures are found around 1590–1600 cm^{-1}, and C–O-containing bands are in the region of 1000–1100 cm^{-1}[40].

Sample B represents the architecture flax/kenaf/flax with no biochar: the contribution of epoxy matrix and treated natural fibres can be distinguished. The spectrum contains bands at approximately 3410, 2922, 1730, 1604, 1506, 1238, 1080, and 830 cm^{-1}. The O–H related region and the C–O containing region are consistent with the contribution of the lignocellulosic fibres, and the aromatic bands around 1604 and 1506 cm^{-1} and the band near 830 cm^{-1} are also consistent with the epoxy matrix. Peaks can be identified around 1730 cm^{-1} as carbonyl-containing groups due to the presence of oxygenated lignocellulosic components[33].

Incorporation of sugarcane-husk biochar in Samples C–F has led to the major spectral regions remaining at the same energies corresponding to combined contribution of epoxy matrix, treated flax/kenaf fibres and biochar. The bands corresponding to O–H are observed around 3400, 3384, 3392 and 3406 cm^{-1} respectively for the Samples C, D, E and F, and the aliphatic C–H band is observed around 2912–2920 cm^{-1}. Samples C–F contain a carbonyl related feature at ~ 1726–1730 cm^{-1}. The positions of the aromatic/carbonaceous region were found to be approximately 1602, 1600, 1598, and 1604 cm^{-1} for Samples C–F, respectively, and remain centred around 1600 cm^{-1}. The low-wavenumber C–O containing band is present around 1052–1088 cm^{-1}. The observations show that the overall spectral profile of the resulting biochar-epoxy and biochar-lignocellulosic hybrid composites changes

with the incorporation of biochar, while maintaining the characteristic absorption regions of the epoxy and lignocellulosic phases[41].

The band around 1600 cm^{-1} is especially difficult to interpret. This band is found in both the isolated sugarcane-husk biochar and in Sample A, and is still observed in Samples B–F, so it is not only a band of the biochar. It is better thought of as an overlapping contribution from aromatic structures in the epoxy matrix and aromatic/conjugated carbon structures of the biochar. The same aromatic/conjugated carbon absorption is reported for biochars derived from sugarcane. Similarly, the changes seen in the O–H and C–O containing regions of C–F are not taken to be indicative of a quantitative decrease in the number of functional groups. No internal standard was used for normalization of spectra and changes in band intensity may be due to sample preparation, matrix components and relative contributions of different phases. Hence, the present FTIR result only identifies the functional-group regions and qualitative changes in their spectral profile and does not quantify the functional-group concentrations. This interpretation is in line with the reviewer's concern that intensity changes may be partly due to compositional or dilution effects[42].

Overall, the FTIR analysis shows that the hybrids developed are also composed of the spectra of LY556/HY951 epoxy matrix, alkali-treated flax fibres, alkali-treated kenaf fibres, and sugarcane-husk biochar. The major regions of O–H, C–H, carbonyl, aromatic/carbonaceous and C–O containing regions are distinguished using the reference spectra. These spectral changes observed support changes in the chemical environment of the composite after biochar incorporation, but the FTIR data cannot be used to confirm hydrogen bonding, better interfacial adhesion, stress transfer, decrease of hydrophilicity or moisture resistance. Other aspects are therefore only mentioned here in connection with the mechanical and SEM findings and not directly from the FTIR spectra.

Mechanical properties

Table 3 presents a summary of mechanical properties of the fabricated flax/kenaf/sugarcane-biochar hybrid composites. The results are expressed as mean ± standard deviation with three specimens tested (n = 3) for each mechanical characterization. The following properties were evaluated: tensile strength, tensile modulus, elongation, flexural strength, flexural modulus, impact strength, hardness and interlaminar shear strength (ILSS). The neat epoxy specimen (Sample A) was prepared using the same epoxy resin (LY556) and hardener (HY951) system as the hybrid composites and was processed and cured under the same conditions, and was used as the experimental baseline. Samples B–F are the flax/kenaf/flax composites containing 0, 1.5, 3, 4.5, and 6 wt% sugarcane biochar, respectively.

Tensile properties

Results showed that tensile strength, tensile modulus, and elongation at break of developed flax/kenaf/flax hybrid composites showed different trends when sugarcane biochar was added. In general, the tensile strength and tensile modulus increased as the biochar content increased up to 4.5 wt%, while the elongation at break showed

Table 3 Mechanical properties of flax/kenaf/sugarcane biochar-based hybrid composites.

Sl. No	Symbol	Tensile strength (MPa)	Tensile modulus (GPa)	Elongation (%)	Flexural strength (MPa)	Flexural modulus (GPa)	Impact strength (kJ/m^2)	Hardness (Shore D)	ILSS (MPa)
1	A	21.88 ± 0.30	1.25 ± 0.04	2.29 ± 0.08	48.48 ± 0.52	2.10 ± 0.05	2.62 ± 0.10	72 ± 1	6.22 ± 0.10
2	B	24.76 ± 0.37	1.85 ± 0.05	3.28 ± 0.16	54.34 ± 0.50	2.75 ± 0.10	5.25 ± 0.25	75 ± 1	8.77 ± 0.25
3	C	25.95 ± 0.38	2.10 ± 0.10	4.17 ± 0.15	59.02 ± 0.55	3.10 ± 0.10	6.56 ± 0.25	78 ± 1	9.11 ± 0.20
4	D	31.48 ± 0.50	2.85 ± 0.15	7.56 ± 0.35	66.97 ± 0.80	3.95 ± 0.15	7.87 ± 0.35	82 ± 1	11.82 ± 0.30
5	E	38.01 ± 0.55	3.60 ± 0.20	3.16 ± 0.15	76.12 ± 0.90	4.80 ± 0.20	9.62 ± 0.45	86 ± 1	13.24 ± 0.35
6	F	27.55 ± 0.60	2.40 ± 0.20	4.18 ± 0.20	58.36 ± 1.00	3.20 ± 0.20	7.21 ± 0.40	80 ± 1	10.80 ± 0.40

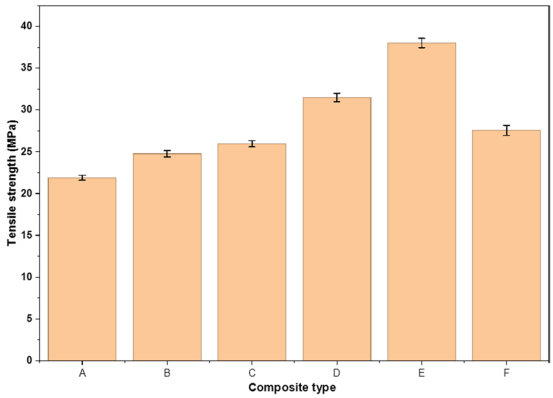


Fig. 10 Tensile strength of flax/kenaf/flax hybrid composites containing different concentrations of sugarcane biochar. Error bars represent standard deviation (n = 3).

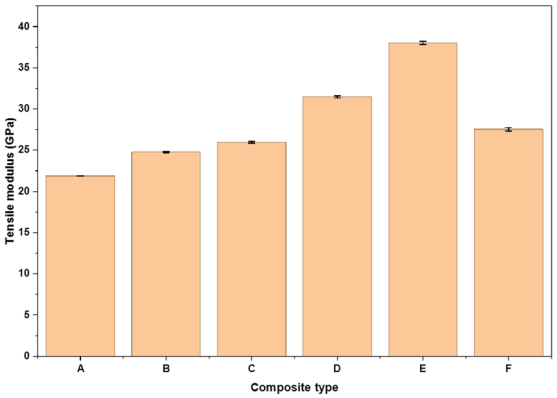


Fig. 11 Tensile modulus of flax/kenaf/flax hybrid composites containing different concentrations of sugarcane biochar. Error bars represent standard deviation (n = 3).

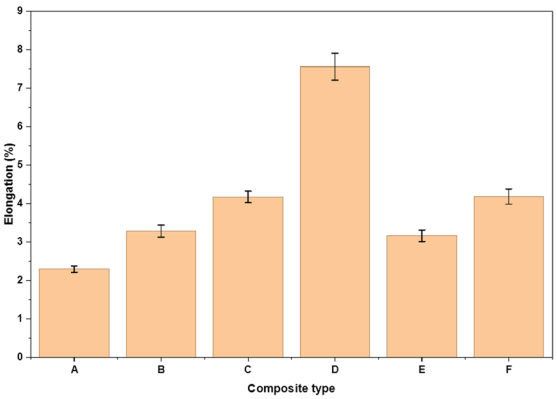


Fig. 12 Elongation at break of flax/kenaf/flax hybrid composites containing different concentrations of sugarcane biochar. Error bars represent standard deviation (n = 3).

non-linear behavior. The results show that the biochar loading affected the load bearing performance and deformation aspect of the hybrid composite system.

The tensile strength of Samples A—F is shown in Fig. 10. The neat epoxy specimen (Sample A) had tensile strength of 21.88 ± 0.30 MPa while the flax/kenaf/flax composite without biochar (Sample B) had tensile strength of 24.76 ± 0.37 MPa, which is an increase of about 13.2%. The tensile strength of the biochar-treated samples showed further improvement with the incorporation of biochar, Sample C with 1.5 wt. % biochar was 25.95 ± 0.38 MPa and Sample D with 3 wt. % biochar was 31.48 ± 0.50 MPa. Sample E with 4.5 wt% biochar had the highest tensile strength (38.01 ± 0.55 MPa) which was about 53.5% higher than that of Sample B and 73.7% higher than Sample A. The progressive increase in the tensile strength of the samples B, C, D and E show that the tensile load bearing response increases as the biochar content is increased in this loading range. The contribution

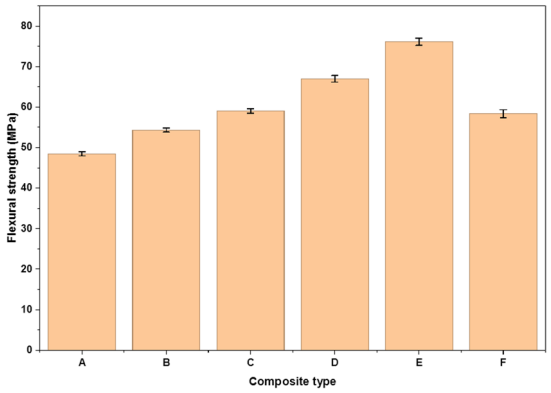


Fig. 13 Flexural strength of flax/kenaf/flax hybrid composites containing different concentrations of sugarcane biochar. Error bars represent standard deviation (n = 3).

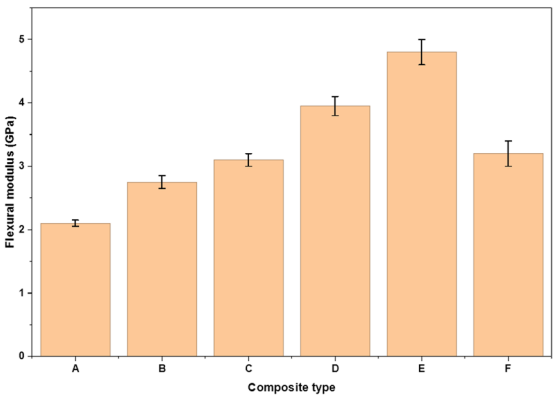


Fig. 14 Flexural modulus of flax/kenaf/flax hybrid composites containing different concentrations of sugarcane biochar. Error bars represent standard deviation (n = 3).

can be related to the introduction of the rigid carbonaceous filler in the epoxy matrix and its interaction with the fibre-reinforced architecture[43]. Since the dispersion of filler and the interfacial properties were not assessed quantitatively in the present study, however, these are thought to be contributing factors but not direct mechanisms[44].

The tensile strength of the composite was reduced to 27.55 ± 0.60 MPa at 6 wt% biochar (Sample F), which is about 27.5% less than that of Sample E. A decline was observed at the highest investigated loading which indicates that there was no further improvement by increasing the biochar incorporation. This composition dependent behaviour can be correlated with the changes in filler distribution and microstructural heterogeneity, as the discussion presented below will indicate, at higher filler loadings. The overall tensile strength was greatest for Sample E of the formulations investigated.

The tensile modulus of the developed composites is shown in Fig. 11. As the biochar content increased, the tensile modulus also increased from 1.25 ± 0.04 GPa for Sample A to 1.85 ± 0.05 GPa for Sample B, 2.10 ± 0.10 GPa for Sample C, 2.85 ± 0.15 GPa for Sample D, and peaked at 3.60 ± 0.20 GPa for Sample E with 4.5 wt% biochar content. The modulus of Sample E was around ninefold more than Sample B and eighteenfold more than Sample A. The modulus of the composite increased with increasing biochar content, showing progressively increased stiffness of the composite up to 4.5 wt%. The rise in stiffness could be attributed to the presence of a relatively stiff carbonaceous biochar phase embedded in the polymer matrix and the consequent inability of the polymer matrix to deform[45]. The tensile modulus at 6 wt% biochar was found to be 2.40 ± 0.20 GPa, suggesting biochar at 4.5 wt% is sufficient to further improve the stiffness of the composite material. Therefore, the formulation of sample E had the highest tensile modulus of all samples analyzed.

The elongation-at-break behaviour varied from the trends of tensile strength and tensile modulus as seen in Fig. 12. Samples C and D had elongation values of 4.17 ± 0.15% and 7.56 ± 0.35% respectively, showing a further increase in elongation. The value of Sample D is about 130.5% greater than that of Sample B. The elongation however, dropped significantly to 3.16 ± 0.15% at 4.5 wt% biochar in Sample E. The elongation was again

increased at 6 wt% (Sample F) to 4.18 ± 0.20%. This non-linear response indicated that the deformation behaviour was found to be different from that of tensile strength and modulus. Sample E was more stiffness-dominated in its tensile response as it has a much higher tensile strength and modulus, as shown by the lower elongation. The behaviour of this sample was found to be different from what had been seen in the other samples, as the deformation behaviour did not only depend on the global stiffness of the composite (Sample F increased). The cause of this non-linear elongation response cannot be definitely determined from the tensile data alone because none of these factors (filler dispersion, local defects or interfacial characteristics) was measured quantitatively[46].

In general, the tensile tests showed that the formulation with 4.5 wt. % biochar (Sample E) gave the highest tensile strength and the lowest elongation at break, while the formulation with 3 wt. % biochar (Sample D) gave the highest elongation at break. The difference between these loadings demonstrates that the loading which led to the greatest strength and stiffness was not same as that which led to greatest deformation capacity.

Flexural properties

The flexural strength and flexural modulus of the developed flax/kenaf/flax hybrid composites are shown in Figs. 13 and 14, respectively. The responses of both properties to the incorporation of sugarcane biochar were composition dependent, with the values increasing up to the maximum of 4.5 wt% investigated and then decreasing at 6 wt% loading of sugarcane biochar.

The flexural strength of the samples A–F is shown in Fig. 13. The flexural strength of the neat epoxy specimen (Sample A) obtained was 48.48 ± 0.52 MPa while that of the flax/kenaf/flax hybrid composite without biochar (Sample B) was 54.34 ± 0.50 MPa which is an improvement of around 12.1%. Sample D, which was prepared by adding 3 wt% biochar, showed an increase in flexural strength to 66.97 ± 0.80 MPa, representing an enhancement of around 23.2% compared with Sample B. Sample C, prepared with 1.5 wt% biochar, demonstrated an increase in flexural strength to 59.02 ± 0.55 MPa, which was an 8.6% enhancement compared with Sample B. The biochar with 4.5 wt% (Sample E) achieved the maximum flexural strength of 76.12 ± 0.90 MPa. This is about 40.1% more than in Sample B.

The flexural strength improved with the addition of biochar up to 4.5 wt%, suggesting that the bending load-bearing property of the hybrid composite has improved in the range of loading investigated. The natural-fibre reinforcement provides the main load-bearing structure, and the rigid biochar phase embedded in the epoxy matrix can also help resist the bending deformations of the matrix[47]. The fibre architecture, therefore, in combination with the incorporation of biochar leads to increasing flexural strength as the biochar content increases from B to E. The flexural results, however, do not provide sufficient information to determine the specific role that interfacial bonding or filler dispersion plays and is evaluated with the morphological observations described below. Flexural strength was found to decrease to 58.36 ± 1.00 MPa at 6 wt% biochar (Sample F), which was about 23.3% lower than that of the Sample E. The reduction indicates that increasing the biochar content from 4.5 to 6 wt% did not provide any further improvement in flexural performance. This decrease is partly attributed to changes of filler distribution and homogeneity at the higher loading, supported by the SEM observations, used to interpret this behaviour[43]. Overall, the highest flexural strength was found in Sample E, among the investigated formulations.

The flexural modulus of developed composites is shown in Fig. 14. The neat epoxy (Sample A) had a flexural modulus of 2.10 ± 0.05 GPa while the flexural modulus of Sample B was 2.75 ± 0.10 GPa, which is a 31.0% improvement after adding the flax/kenaf/flax reinforcement. This was followed by an increase of the flexural modulus to 3.10 ± 0.10 GPa and 3.95 ± 0.15 GPa for Sample C and Sample D, respectively. The highest value of 4.80 ± 0.20 GPa was observed for Sample E with 4.5 wt. % biochar. This is about 74.5% more than Sample B, and 128.6% more than the neat epoxy (Sample A). The flexural modulus was observed to increase with the amount of biochar, suggesting an increase in resistance to elastic deformation under bending stress, up to 4.5 wt%. The relatively stiff carbonaceous biochar particles may increase the stiffness of the epoxy rich matrix, and the flax/kenaf reinforcement is also structurally stiff. This is expected as the contribution of the biochar phase is

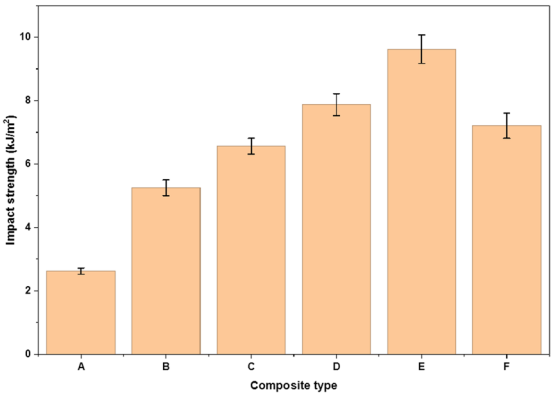


Fig. 15 Impact strength of flax/kenaf/flax hybrid composites containing different concentrations of sugarcane biochar. Error bars represent standard deviation (n = 3).

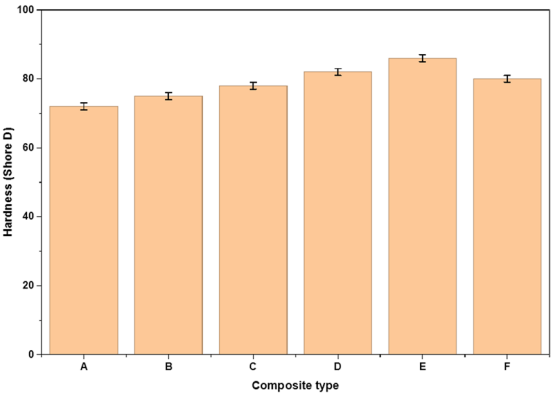


Fig. 16 Shore D hardness of flax/kenaf/flax hybrid composites containing different concentrations of sugarcane biochar. Error bars represent standard deviation (n = 3).

increased from Sample B to Sample E, which is consistent with the progression observed in each of the stiffness measurements. Flexural modulus value for biochar at 6 wt% (Sample F) was 3.20 ± 0.20 GPa which is around 33.3% less than that of Sample E. The reduction suggests that there was no additional increase in flexural stiffness at the highest investigated biochar loading. The reduction could be due to redistribution of the filler and the local structural heterogeneity at high loading and not be clearly attributed to any one mechanism without direct microstructural evidence.

In general, flexural properties show that the flexural strength and flexural modulus are the highest for the formulation of Sample E (4.5 wt. % biochar). The subsequent drop at 6 wt% suggests that adding any more biochar to the mixture was detrimental for flexural response under these experimental conditions.

Impact strength

The impact strength of the developed flax/kenaf/flax hybrid composites with different sugarcane biochar loadings is presented in Fig. 15. The impact strength was found to increase with increasing biochar loading from Samples B to E and then declined at the highest biochar loading studied. The impact strength of Sample B (flax/kenaf/flax without biochar) was 5.25 ± 0.25 kJ/m^2, which was higher than the neat epoxy (Sample A) by around 100.4%. This rise shows that the energy absorption capability of the composite under impact loading can be attributed to the flax/kenaf fibre architecture. The impact strength further improved with the incorporation of 1.5 wt% biochar, Sample C, to 6.56 ± 0.25 kJ/m^2, an improvement of approximately 24.9% relative to Sample B. The incorporation of 3 wt% biochar (Sample D), significantly increased the impact strength to 7.87 ± 0.35 kJ/m^2 (approximately 49.9% relative to Sample B).

The sample with 4.5 wt% of biochar (Sample E) had the highest impact strength of 9.62 ± 0.45 kJ/m^2. This is about 83.2% more than in Sample B and 267.2% more than the neat epoxy (Sample A). The reinforcing

architecture of biochar/flax, along with the gradual increase in impact strength up to 4.5 wt% of biochar, improved the energy absorption performance under the current impact-testing conditions. The observed improvement may be related to the synergistic effect of the fracture-energy dissipation provided by the fibre-reinforced structure and the carbonaceous filler[23]. The impact results do not directly reveal mechanisms such as crack deflection, fibre pull-out, or changes in interfacial adhesion; these aspects are therefore interpreted in conjunction with the subsequent SEM observations. The impact strength decreased to 7.21 ± 0.40 kJ/m^2 (around 25.1% less than Sample E) at 6 wt. % biochar (Sample F). This reduction suggests that there was no further improvement in impact resistance when more than 4.5 wt% biochar was added. The distribution of fillers and the local heterogeneity at higher loading can play a role in the observed decrease in energy absorption, as well as the morphology of the fracture, which is provided by the subsequent observations in the SEM.

In general, the results indicated that Sample E (4.5 wt% biochar) had the highest impact strength among the samples studied. At this loading, maximum energy absorbed at impact occurred despite the lower elongation at the point of break in the tensile test, demonstrating that impact energy absorption is not solely related to the tensile ductility of the hybrid composite, but is also influenced by the overall fracture response of the hybrid composite.

Hardness

In this regard, the Shore D hardness values of developed flax/kenaf/flax hybrid composites with different concentrations of sugarcane biochar are shown in Fig. 16. The hardness showed an increasing trend up to 4.5 wt% biochar and thereafter a decreasing trend at 6 wt% biochar. The neat epoxy sample (Sample A) had a hardness of 72 ± 1 Shore D while the sample without biochar of flax/kenaf/flax composite (Sample B) had a hardness of 75 ± 1 Shore D, which is about 4.2% higher than that of the neat epoxy sample. This increase represents the contribution of the natural fibre reinforcement to the surface resistance of the hybrid composite. The addition of 1.5 wt% biochar resulted in a higher hardness of Sample C (78 ± 1 Shore D) and 3 wt% biochar resulted in a higher hardness for Sample D (82 ± 1 Shore D).

The composite contains 4.5 wt% of biochar in Sample E gave the highest hardness of 86 ± 1 Shore D. This is about 14.7% higher than the value of Sample B and 19.4% higher than the neat epoxy (Sample A). Progressive increase in hardness with biochar incorporation is an increase in resistance to localized indentation under present test conditions. The carbonaceous biochar phase is relatively rigid and could be responsible for the higher surface stiffness of the composite, and the flax/kenaf reinforcement also gave greater resistance to local deformation. Thus, the observed trend would be consistent with the trend of the increasing contribution of the reinforcing phases to the surface hardness of the composite[43,48]. The hardness of sample F at 6 wt% biochar was reduced to 80 ± 1 Shore D, which was about a 7.0% drop compared to that of Sample E. The reduction suggests that the biochar fraction above 4.5 wt% does not provide any further improvement in hardness. The decrease in the higher concentration of the filler may be due to changes in the distribution and the local heterogeneity; however,

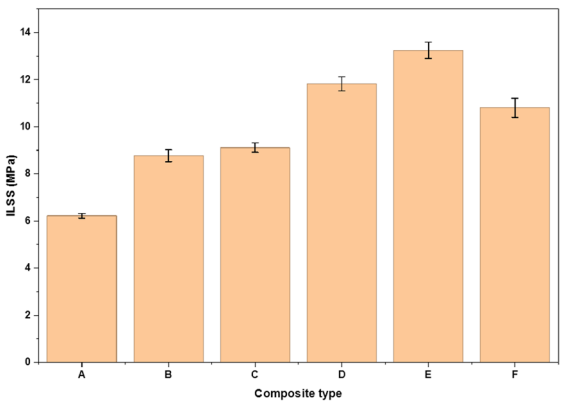


Fig. 17 Interlaminar shear strength of flax/kenaf/flax hybrid composites containing different concentrations of sugarcane biochar. Error bars represent standard deviation (n = 3).

Table 4 One-way ANOVA results showing the effect of biochar concentration on the mechanical properties of flax/kenaf/flax hybrid composites.

Property	F-value	p-value
Tensile strength (MPa)	439.07	<0.001
Tensile modulus (GPa)	102.77	<0.001
Elongation (%)	250.52	<0.001
Flexural strength (MPa)	511.71	<0.001
Flexural modulus (GPa)	128.54	<0.001
Impact strength (kJ/m^2)	165.32	<0.001
Hardness (Shore D)	74.9	<0.001
ILSS (MPa)	228.44	<0.001

Table 5 Tukey HSD grouping of mechanical properties of flax/kenaf/flax hybrid composites.

Sample	Tensile strength (MPa)	Tensile modulus (GPa)	Elongation (%)	Flexural Strength (MPa)	Flexural Modulus (GPa)	Impact Strength (kJ/m^2)	Hardness (Shore D)	ILSS (MPa)
A	21.88 ± 0.30^{e}	1.25 ± 0.04^{e}	2.29 ± 0.08^{d}	48.48 ± 0.52^{e}	2.10 ± 0.05^{e}	2.62 ± 0.10^{e}	72 ± 1^{e}	6.22 ± 0.10^{e}
B	24.76 ± 0.37^{d}	1.85 ± 0.05^{d}	3.28 ± 0.16^{c}	54.34 ± 0.50^{d}	2.75 ± 0.10^{d}	5.25 ± 0.25^{d}	75 ± 1^{d}	8.77 ± 0.25^{d}
C	25.95 ± 0.38^{d}	2.10 ± 0.10^{cd}	4.17 ± 0.15^{b}	59.02 ± 0.55^{c}	3.10 ± 0.10^{cd}	6.56 ± 0.25^{c}	78 ± 1^{c}	9.11 ± 0.20^{d}
D	31.48 ± 0.50^{b}	2.85 ± 0.15^{b}	7.56 ± 0.35^{a}	66.97 ± 0.80^{b}	3.95 ± 0.15^{b}	7.87 ± 0.35^{b}	82 ± 1^{b}	11.82 ± 0.30^{b}
E	38.01 ± 0.55^{a}	3.60 ± 0.20^{a}	3.16 ± 0.15^{c}	76.12 ± 0.90^{a}	4.80 ± 0.20^{a}	9.62 ± 0.45^{a}	86 ± 1^{a}	13.24 ± 0.35^{a}
F	27.55 ± 0.60^{c}	2.40 ± 0.20^{c}	4.18 ± 0.20^{b}	58.36 ± 1.00^{c}	3.20 ± 0.20^{c}	7.21 ± 0.40^{bc}	80 ± 1^{bc}	10.80 ± 0.40^{c}

the mechanism cannot be inferred from the hardness measurements alone and it is parallel to the morphological observations.

In general, the hardness test results indicate that the formulation containing 4.5 wt% biochar had the highest Shore D hardness value among the formulations tested. The reduction at 6 wt% further indicates the increasing the biochar content beyond 4.5 wt% was not beneficial for surface hardness under the conditions of this experiment.

ILSS

Figure 17 shows the interlaminar shear strength (ILSS) of the various flax/kenaf/flax hybrid composites with different percentages of sugarcane biochar. The flax/kenaf/flax laminate architecture is used in Samples B–F and the comparison in this section is limited to these samples. The unfilled flax/kenaf/flax composite (Sample B) had an ILSS value of 8.77 ± 0.25 MPa. The ILSS value for the sample with 1.5 wt% biochar (Sample C) was 9.11 ± 0.20 MPa, which is about 3.9% higher than for Sample B. The sample with 3 wt% biochar (Sample D) had an ILSS of 11.82 ± 0.30 MPa, an improvement of approximately 34.8% compared to that of Sample B. This gradual rise suggests biochar incorporation was linked to an improvement of the measured resistance to interlaminar shear within the range of biochar content investigated.

Sample E (4.5 wt% biochar) showed the highest ILSS value of 13.24 ± 0.35 MPa. This is about 50.9% higher when compared with the unfilled flax/kenaf/flax composite (Sample B). The improvement indicates that biochar contents up to 4.5 wt% improved the shear-bearing response of the hybrid laminate under the current test conditions. Interlaminar modification has similarly been reported to improve the apparent interlaminar shear and fracture response of fibre-reinforced epoxy laminates[49]. The stiffness of the resin-rich areas between the fibre layers could be affected by the rigid carbonaceous filler, which may affect the resistance of the laminate to interlaminar shear deformation[24,50]. The present ILSS tests, however, do not provide any evidence for specific mechanisms.

The ILSS was further reduced to 10.80 ± 0.40 MPa at 6 wt% biochar (Sample F) which is about 18.4% less than Sample E. The reduction shows that more than 4.5 wt% of biochar did not improve the interlaminar shear performance. The observed reduction is likely to be due to changes in filler distribution and/or local heterogeneity at the higher loading but these cannot be definitively concluded from the ILSS results.

It can be concluded from overall results of the ILSS test that the formulation of 4.5 wt% biochar in the sample E has the highest ILSS compared to the other flax/kenaf/flax formulations tested. The following decrease at 6 wt% shows that the ILSS response is composition dependent, with further addition of biochar not leading to any further enhancement of interlaminar shear properties.

Statistical analysis

Means ± standard deviation (SD) are given for mechanical-property measurements, which were obtained from three separate specimens (n = 3). One-way analysis of variance (ANOVA) was used to compare the mechanical properties measured for the different composite formulations that were tested. If this difference was found to be significant overall, a Tukey's honestly significant difference (HSD) post hoc test was conducted at the $p < 0.05$ significance level for the pairwise comparisons[51]. Error bars shown in the respective figures are the standard deviation of the three measurements. The results of the ANOVA are given in Table 4 and Tukey HSD grouping results in Table 5.

Table 4 summarizes the results of the one-way ANOVA for the eight mechanical properties investigated, indicating that they were statistically significantly different for all formulations ($p < 0.001$). The F-values for tensile strength, tensile modulus, elongation at break, flexural strength, flexural modulus, impact strength, hardness, and ILSS were 439.07, 102.77, 250.52, 511.71, 128.54, 165.32, 74.90 and 228.44, respectively. The results show that the composite formulation and the different concentrations of biochar caused a significant difference in the mechanical response measured.

The results of the ANOVA were followed by Tukey's HSD post hoc analysis to determine the differences among individual formulations. Table 5 shows the corresponding statistical groupings. Significant differences between samples are denoted by different superscript letters and samples having one or more common letter are not significantly different at $p < 0.05$.

The results revealed that the differences were statistically significant ($p < 0.05$) according to the Tukey tests (Table 5) depending on the property and biochar concentration. The tensile strength increased from 21.88 ± 0.30 MPa (Sample A) to 38.01 ± 0.55 MPa (Sample E) and then decreased to 27.55 ± 0.60 MPa (Sample F). The tensile strength values of Samples B and C were not significantly different, as indicated by their shared Tukey grouping, whereas Sample A differed significantly from Samples B and C ($p < 0.05$). The values obtained for the higher loading formulation (Samples D and E) were, however, statistically different from the lower loading formulations with the Tukey grouping. The overall trend of tensile modulus was similar, with Sample A having a mean of 1.25 ± 0.04 GPa, and Sample E having a mean of 3.60 ± 0.20 GPa, with Sample B and Sample C showing a similar mean value, and Sample C and Sample F showing a similar Tukey grouping. As a result, the mean tensile modulus increased as the amount of biochar was added, but not all additions of biochar were statistically different from one another.

The flexural properties showed a significant improvement up to Sample E which was 48.48 ± 0.52 MPa for Sample A and 76.12 ± 0.90 MPa for Sample E, while flexural modulus increased from 2.10 ± 0.05 GPa to 4.80 ± 0.20 GPa. Sample F decreased in both properties after. Samples C and F had the same Tukey grouping for flexural strength, meaning that there was no significant difference between these two formulations at $p < 0.05$. The statistical behaviour of impact strength and hardness were similar. The impact strength of Sample F was lower than that of Sample E, but there were statistically similar impact strength values as indicated by the Tukey groupings between the two samples for certain comparisons; the hardness of Sample F was also reduced as compared to Sample E, though some pairwise comparisons between Sample F and other samples were not statistically different as indicated by the shared Tukey groupings.

The comparison is made between the formulations of ILSS and the formulations of the other flax/kenaf/flax formulations (Samples B–F). The difference between the ILSS of samples B and C was not statistically significant ($p > 0.05$), while the higher loading levels had statistically significant differences by Tukey grouping. Elongation had an opposite trend to the other mechanical properties. The maximum value was obtained for Sample

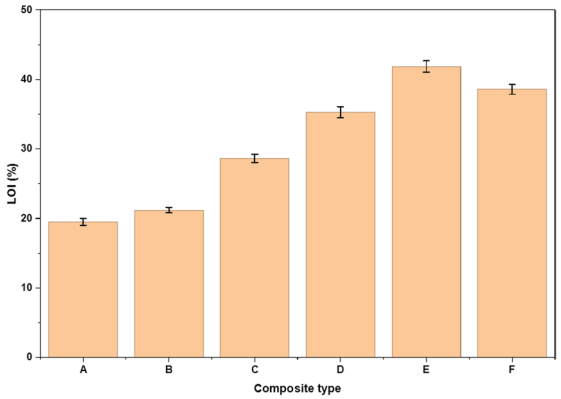


Fig. 18 LOI of flax/kenaf/sugarcane biochar-based hybrid composites

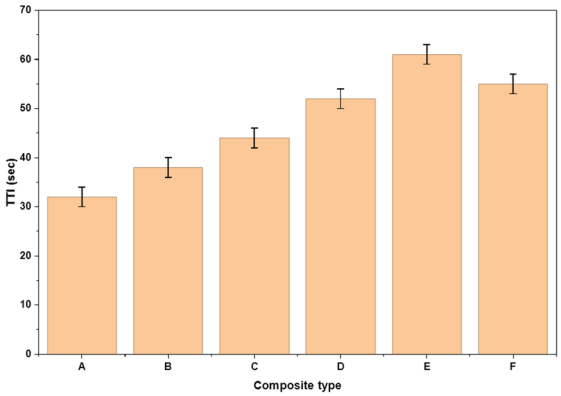


Fig. 19 Time to ignition (TTI) of flax/kenaf/flax hybrid composites containing different concentrations of sugarcane biochar.

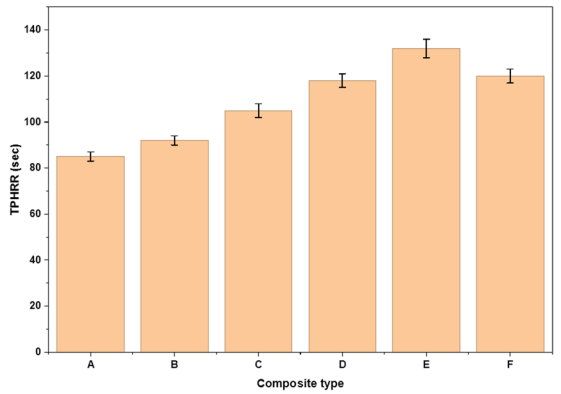


Fig. 20 Time to peak heat release rate (TPHRR) of flax/kenaf/flax hybrid composites containing different concentrations of sugarcane biochar.

D (7.56±0.35%), whereas Sample E decreased to 3.16±0.15%. Samples B and E were found to be statistically equal as were samples C and F by the Tukey grouping. So, it is not correct to say that the 4.5 wt% biochar formulation is the one that makes the maximum elongation.

Overall, the combined ANOVA and Tukey analyses show that the composite formulation had a statistically significant effect on all mechanical properties investigated. The post-hoc analysis, however, shows that some differences between the consecutive formulations were not statistically significant. Sample E (4.5wt%) biochar) had the highest tensile strength, tensile modulus, flexural strength, flexural modulus, impact strength, hardness and ILSS measured, while Sample D had the highest elongation measured. Thus, the statistical analysis suggests that the formulation included in Sample E affords the highest overall balance of mechanical properties, and that there are property specific differences and formulations that are statistically comparable.

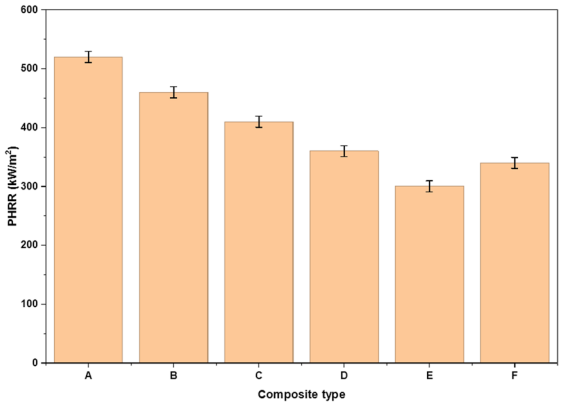


Fig. 21 Peak heat release rate (PHRR) of flax/kenaf/flax hybrid composites containing different concentrations of sugarcane biochar.

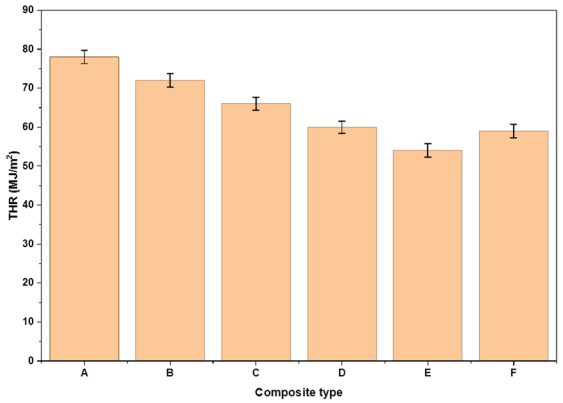


Fig. 22 Total heat release rate (THR) of flax/kenaf/flax hybrid composites containing different concentrations of sugarcane biochar.

Fire-performance characteristics

Limiting oxygen index (LOI)

The Limiting Oxygen Index (LOI) results indicate that flame retardancy improves with the addition of sugarcane biochar and both fiber reinforcements. The neat epoxy composite (Sample A) has the lowest LOI of 19.5%, indicating high flammability and easy combustion under normal air conditions. The LOI improves by about 8.7% over plain epoxy to 21.2±0.4% (Sample B) for the flax/kenaf/flax fiber composite without biochar. The primary reason for this increase may be associated with the formation of carbonaceous residue from the natural fibres during combustion[52]. A more noteworthy improvement occurs with the addition of sugarcane biochar. The LOI increases to 23.6±0.6% at 1.5 wt% biochar (Sample C), which is about 21% higher than pure epoxy. The LOI further increases to 25.8±0.8% at 3 wt% biochar (Sample D). The increase in LOI with biochar incorporation is consistent with increased formation of carbonaceous residue, which may contribute to a protective condensed-phase structure during combustion[25]. At 4.5 wt% biochar (Sample E), the LOI reaches 28.4±0.8%, which is about 45.6% higher than that of neat epoxy, may be associated with the presence of sugarcane biochar. The results indicate that biochar incorporation is associated with increased char formation, which may contribute to the observed improvement in flame resistance. Figure 18 shows the LOI values of waste sugarcane husk-based hybrid composites.

The carbon-rich structure of biochar may contribute to the formation of a more continuous carbonaceous residue, which may restrict the release of volatile degradation products during combustion[25]. At 6 wt% biochar, the LOI value slightly decreases to 26.7±0.7%, which is still about 36.9% higher than that of neat epoxy. The reduction observed at 6 wt%, compared to 4.5 wt%, suggests that increasing biochar concentration may lead to

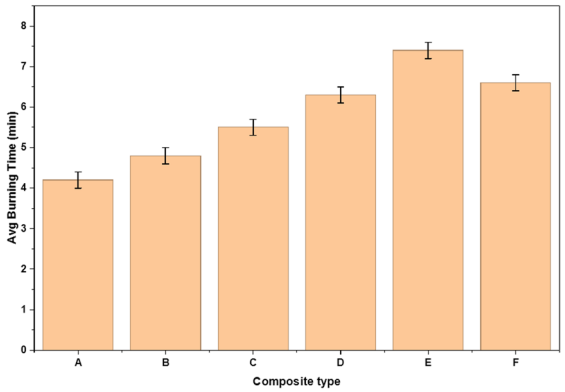


Fig. 23 Average burning time of flax/kenaf/flax hybrid composites containing different concentrations of sugarcane biochar. Error bars represent standard deviation (n = 3).

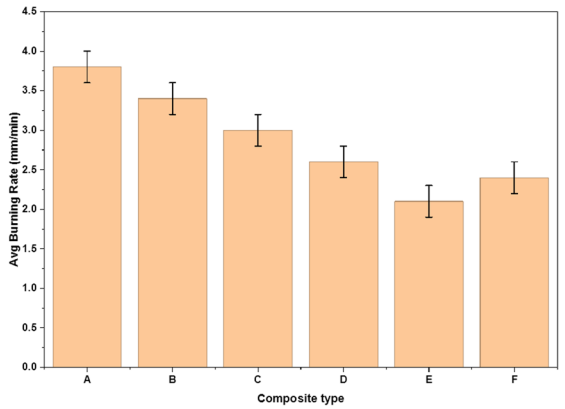


Fig. 24 Average burning rate of flax/kenaf/flax hybrid composites containing different concentrations of sugarcane biochar. Error bars represent standard deviation (n = 3).

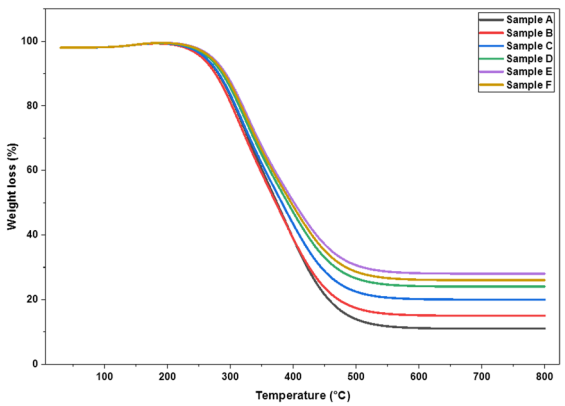


Fig. 25 TGA curves of flax/kenaf/flax hybrid composites containing different concentrations of sugarcane biochar.

inadequate dispersion and the formation of particle clusters within the epoxy matrix. These clusters can form defects, especially at the interfaces, and can also compromise the continuity of the protective char layer, causing a slight decrease in fire resistance performance[53]. Thus, the biochar obtained from sugarcane and mixed with hybrid fiber reinforcement enhances the LOI. The flame resistance effect is best at 4.5 wt% biochar, emphasizing the need for well-dispersed biochar, good char integrity, and a stable char barrier.

Cone calorimeter analysis of hybrid composites

The cone calorimeter data give information on the reaction-to-fire behaviour of the flax/kenaf/flax hybrid composites with sugarcane biochar and the neat epoxy reference. Time to ignition (TTI), time to peak heat release

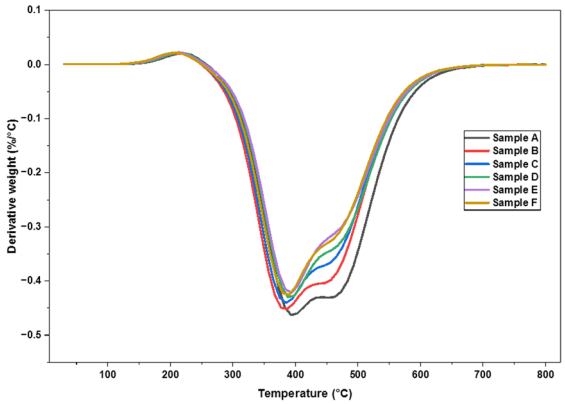


Fig. 26 DTG curves of flax/kenaf/flax hybrid composites containing different concentrations of sugarcane biochar.

Table 6 Thermal degradation parameters of flax/kenaf/flax hybrid composites containing different concentrations of sugarcane biochar.

Sample	Biochar (wt%)	T_{onset} (°C)	T_{max} (°C)	DTG at T_{max}	Residual char (%)
A	0	278	393	−0.4630	11
B	0	293	387	−0.4520	14
C	1.5	303	385	−0.4405	19
D	3	309	388	−0.4300	24
E	4.5	317	394	−0.4215	28
F	6	313	390	−0.4255	25

rate (TPHRR), peak heat release rate (PHRR) and total heat release (THR) were measured. The outcomes show the biochar dose dependency of the fire response.

The time to ignition (TTI) values are given in Fig. 19. The neat epoxy specimen (Sample A) had a TTI of 32 ± 2 s while the unfilled flax/kenaf/flax composite (Sample B) had an increased TTI of 38 ± 2 s. With increasing biochar content, the TTI increased to 44 ± 2 s for Sample C (1.5 wt%), 52 ± 2 s for Sample D (3 wt%), and reached 61 ± 2 s for Sample E (4.5 wt%). Sample F (6 wt. % biochar) had a reduced TTI of 55 ± 2 s. The TTI of Sample E increased by about 90.6% compared with Sample A. The trend of TTI increasing until Sample E suggests that there is a lag in ignition as the biochar level increases in the range investigated[25]. The thermal degradation properties derived from the TGA/DTG analysis are consistent with this behaviour, as the onset degradation temperature in the analysis increased from 278 °C for Sample A to 317 °C for Sample E, with an increase in the amount of residual char from 11 to 28%. These changes mean high thermal stability and high thermally stable carbonaceous residue formation at the loading of 4.5 wt. % biochar. In the present study, however, the thermal conductivity was not measured directly and is thus not attributed to a reduction in thermal conductivity.

The time to peak heat release rate (TPHRR) is shown in Fig. 20. TPHRR increased from 85 ± 2 s for Sample A to 92 ± 2 s for Sample B and further to 105 ± 3 s, 118 ± 3 s, and 132 ± 4 s for Samples C, D, and E, respectively. Hence, the maximum TPHRR was recorded for the Sample E which had 4.5 wt% biochar. Delayed appearance of the maximum heat-release rate suggests that the maximum heat-release event is happening later in the cone calorimeter test. This behaviour is similar to the modified thermal degradation behaviour observed in the TGA/DTG analysis, such as the increase in onset degradation temperature, and the change in the main degradation characteristics by adding biochar. This increase up to 4.5 wt% was not sustained at higher filler loadings as Sample F had a TPHRR of 120 ± 3 s at 6 wt% biochar.

The peak heat release rates (PHRR) are shown in Fig. 21. PHRR decreased progressively from 519.98 ± 9.53 kW/m^2 for Sample A to 460.02 ± 9.45 kW/m^2 for Sample B, 410.05 ± 9.37 kW/m^2 for Sample C, 360.01 ± 9.26 kW/m^2 for Sample D, and 300.10 ± 9.28 kW/m^2 for Sample E. Thus, Sample E exhibited a reduction of approximately 42.3% in PHRR compared with the neat epoxy reference. The decrease in PHRR indicates a lower maximum rate of heat release during combustion with increasing biochar content up to 4.5 wt%. This behaviour is in line with the increase in the residual char (11% to 28%) seen in the TGA analysis of the various samples[54]. This larger

percentage of the carbonaceous fraction could result in a condensed phase residue being formed and thus affect the degradation product volatiles released during the thermal process. The present study, however, did not directly measure the thermal-barrier effect or thermal conductivity of the residue and therefore these are considered as possible mechanisms rather than direct measurements.

At 6 wt% biochar, the PHRR increased to 340.04 ± 9.37 kW/m^2, while TPHRR decreased to 120 ± 3 s and TTI decreased to 55 ± 2 s. The amount of residual char also reduced from 28% for Sample E to 25% for Sample F as a result of the TGA/DTG analysis. The results of simultaneous changes of TTI, TPHRR, PHRR and residual char showed that no further enhancement to the fire performance could be achieved by increasing the amount of biochar beyond 4.5 wt%. The reverse trend observed may be related to the distribution of the filler and the composite structure at the higher loading of biochar; however, this is proposed as a possible explanation and not a directly established mechanism.

The total heat release (THR) values are shown in Fig. 22. THR decreased progressively from 78.02 ± 1.72 MJ/m^2 for Sample A to 71.97 ± 1.73 MJ/m^2, 66.01 ± 1.67 MJ/m^2, 59.98 ± 1.59 MJ/m^2, and 54.03 ± 1.74 MJ/m^2 for Samples B, C, D, and E, respectively. Thus, the lowest THR was found for Sample E which was about 30.7% lower than that of Sample A. The lower value of THR signifies smaller cumulative heat release during cone calorimeter test. At the higher biochar loading of 6 wt%, THR reached 59.02 ± 1.73 MJ/m^2, which shows that the enhancement achieved up to 4.5 wt. % biochar was not sustained at the higher loading. The decrease in THR up to Sample E is consistent with the corresponding decrease in PHRR and increase in the amount of residual char observed in the TG/DTG analysis.

Overall, the cone calorimeter results showed that reaction-to-fire (RTF) properties of the flax/kenaf/flax hybrid composites were gradually altered by the addition of sugarcane biochar up to 4.5 wt%. The TTI and TPHRR were highest for Sample E, whereas the PHRR and THR were lowest among the investigated formulations. The changes observed in the measured cone-calorimeter parameters for Sample F, when the biochar content was increased to 6 wt%, show that further biochar addition did not provide better results for the measured parameters. Cone calorimeter test data are combined with the TGA/DTG data, to conclude that the formulation with 4.5 wt% biochar has the most desirable overall fire-performance response of the formulations tested[55,56].

Horizontal burning characteristics

The burning behavior of the manufactured composites was assessed in terms of burning duration and burning rate in a horizontal direction. The average burning duration increased progressively from 4.2 ± 0.2 min for Sample A to 4.8 ± 0.2, 5.5 ± 0.2, 6.3 ± 0.2, and 7.4 ± 0.2 min for Samples B–E, respectively, as shown in Fig. 23. Therefore, the burning time of Sample E was approximately 76.2% longer than that of a neat epoxy reference. The burning time was slightly reduced to 6.6 ± 0.2 min at 6 wt. % biochar (Sample F). The longer burning time does not necessarily indicate improved fire safety under actual burning conditions and therefore cannot be interpreted as an improvement in fire safety.

Similarly, the average burning rate decreased progressively from 3.8 ± 0.2 mm/min for Sample A to 3.4 ± 0.2, 3.0 ± 0.2, 2.6 ± 0.2, and 2.1 ± 0.2 mm/min for Samples B–E, respectively, as presented in Fig. 24. The burning rate was slightly raised to 2.4 mm/min at 6 wt% biochar. The reduction in burning rate up to 4.5 wt% biochar indicates slower burning under the horizontal burning conditions used in this test. However, the reduction in burning rate was not sustained at 6 wt% biochar, where the burning rate increased slightly to 2.4 mm/min. Increasing the biochar content could alter filler distribution and the composite structure, which may contribute to the observed change in burning behaviour; however, this could not be directly established in the present study[57]. The overall results of horizontal-burning tests are combined with the LOI and cone-calorimeter results to avoid relying exclusively on burning time as a measure of fire performance.

TGA and DTG analysis

To assess the thermal degradation behaviour of the developed flax/kenaf/flax hybrid composites, the thermogravimetric analysis (TGA) and derivative thermogravimetric (DTG) analysis tests were carried out. To investigate the effect of sugarcane biochar incorporation on thermal stability and residual char formation, the TGA and DTG test were performed. Figures 25 and 26 show the TGA and DTG curves, respectively, of the samples A–F, and Table 6 gives the thermal degradation parameters.

The TGA curves of the samples A – F are shown in Fig. 25. The TGA results clearly indicate a change in the thermal degradation behaviour due to the addition of biochar. The T_{onset} value of neat epoxy (Sample A) was 278 °C, while the flax/kenaf/flax composite without biochar (Sample B) resulted in a higher T_{onset} of 293 °C. The T_{onset} values were increased progressively for increasing amounts of biochar to 303 °C for Sample C (1.5 wt. %), 309 °C for Sample D (3 wt. %), and 317 °C for Sample E (4.5 wt. %). Sample F had a slight decrease in T_{onset} (313 °C), while Sample E had the highest T_{onset} (317 °C), which was 39 °C higher than that of Sample A. This change suggests the biochar formulation with 4.5 wt% needed a higher temperature to start the main thermal degradation process. Increased thermal degradation was also observed in biochar-containing epoxy systems, in which the degradation temperatures and thermal stability of the epoxy matrix were altered by the addition of biochar[44].

The dependence of biochar loading was even more evident in terms of the residual char content. The percentage of residual char of the samples increased from 11% for Sample A to 14% for Sample B, and finally to 19%, 24%, and 28% for Samples C, D, and E, respectively. When 6 wt. % biochar was incorporated into the sample, the residual char content for Sample F was reduced slightly to 25%. This means that the incorporation of 4.5 wt% biochar resulted in a 17-percentage-point increase in residual char content compared with Sample A. The gradual increase in the amount of residual char up to 4.5 wt% shows that the biochar composites contain a higher proportion of thermally stable carbonaceous residue. Comparable gains in the residue mass have been observed in biochar-epoxy composites, in which the carbonaceous components gave rise to a higher amount of thermally stable residue following pyrolysis[56,58]. The production of higher amounts of carbonaceous residue has also been linked to greater flame-retardant performance in agricultural-waste based epoxy formulations.

The DTG curves corresponding to these are shown in Fig. 26 and give further details of the rate of mass loss on thermal degradation. The T_{max} values obtained from the minimum DTG values were found to be 393 °C for Sample A, 387 °C for Sample B, 385 °C for Sample C, 388 °C for Sample D, 394 °C for Sample E and 390 °C for sample F. The DTG peak magnitude also decreased progressively from −0.4630 for Sample A to −0.4520, −0.4405, −0.4300, and −0.4215 for Samples B–E, respectively. Sample F showed a slight increase in the peak magnitude to −0.4255. The T_{max} value was not necessarily a monotonically increasing function of biochar loading, but the gradual decrease in the DTG peak size from Sample A to Sample E suggests a smaller maximum mass loss rate in the major degradation region. Sample E was found to have the highest T_{max} (394 °C) and the lowest value of DTG peak (−0.4215). The slight reversal of Sample F is in line with the decrease in T_{onset} and remaining char at the same loading.

The observed DTG behaviour is similar to other reported studies using biochar filled epoxy materials where the addition of carbonaceous fillers altered the DTG profile and degradation behaviour of the epoxy matrix. The thermal decomposition behaviour of epoxy-based composites with various amount of biochar can be altered by the biochar content, which was confirmed previously[38]. This comparison supports the present observation that biochar influences the amount, rate, and temperature characteristics of thermal degradation.

The results of the combined TGA and DTG data were thus found to be most favourable for the biochar formulation 4.5 wt%. Sample E had the highest T_{onset} (317 °C), highest T_{max} (394 °C), highest residual char content (28%), and the lowest principal DTG peak (−0.4215). The results here showed that biochar addition altered the initial temperature of degradation and the amount and rate of mass loss during thermal degradation. The observed behaviour is in line with the presence of thermally stable carbonaceous constituents added by the sugarcane biochar[59].

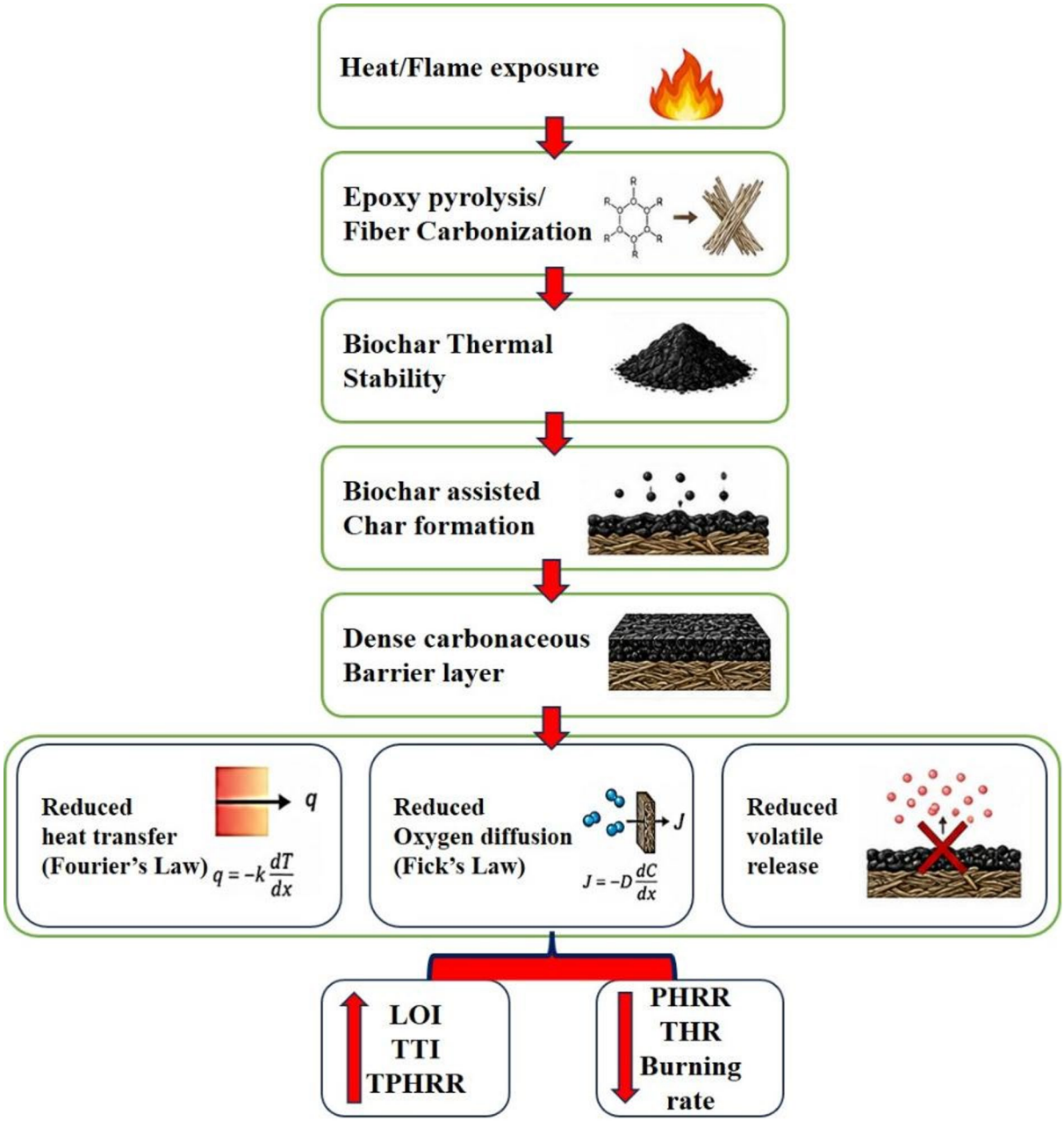


Fig. 27 Proposed condensed-phase flame-retardant mechanism of flax/kenaf/sugarcane biochar hybrid composites.

The decrease in the rate of thermal degradation and the increase in the amount of char is especially significant for the fire-performance behaviour that has been seen from the LOI and cone calorimeter measurements. Increased residual carbonaceous material can affect the condensed phase residue production during combustion and affect the transport of the volatile degradation products and further degradation. This kind of condensed-phase char/barrier effect has been found in the case of biochar-epoxy composites and agricultural-waste-based epoxy-FR systems. In the present TGA/DTG measurements, however, direct measurements of thermal conductivity or quantification of heat transfer resistance was not possible. The protective thermal-barrier effect of the carbonaceous residue is therefore proposed based on the combined TGA/DTG and fire-performance results and was not measured directly in the present study.

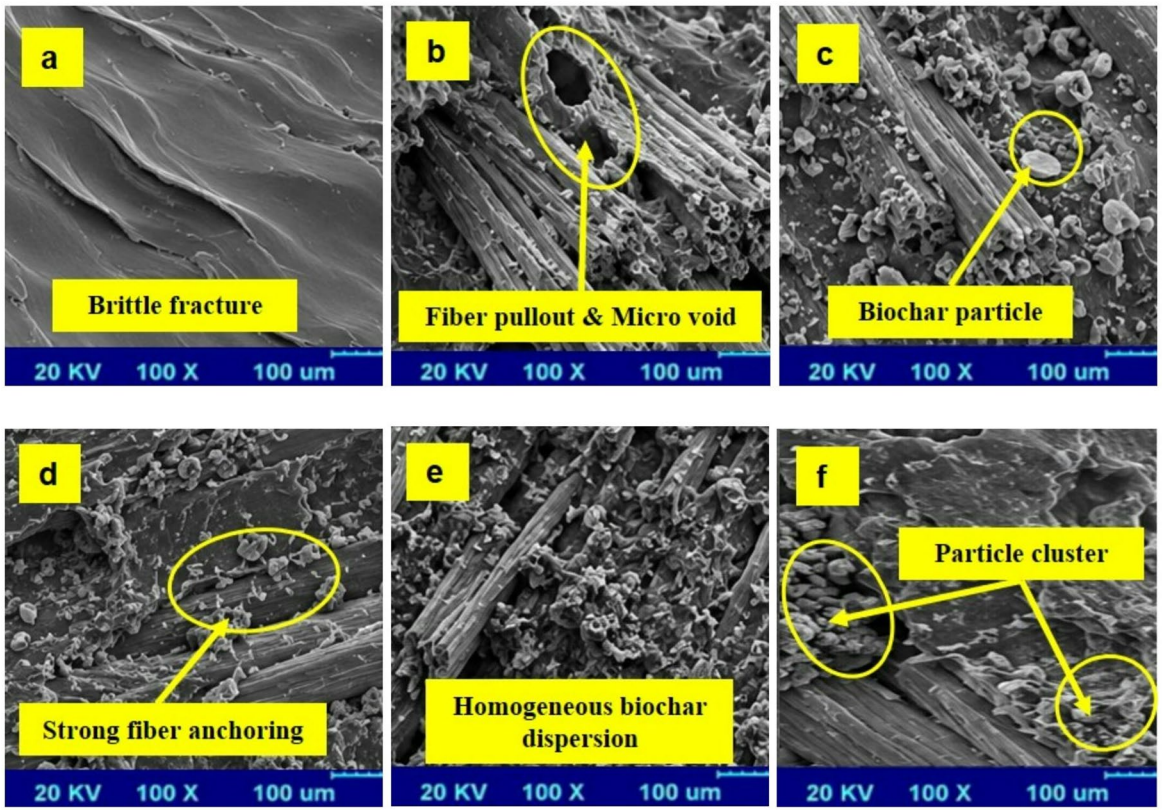


Fig. 28 SEM micrographs of tensile-fractured surfaces of fabricated composites: (**a**) Sample A; (**b**) Sample B; (**c**) Sample C; (**d**) Sample D; (**e**) Sample E; and (**f**) Sample F.

The slight decrease in T_{onset} from 317 °C to 313 °C and residual char from 28 to 25% at 6 wt% biochar also indicates that adding more filler beyond the optimum investigated loading does not necessarily result in a greater protective effect. This behaviour is similar to that which might be expected if the filler distribution and composite structure changed at higher biochar loading. The TGA/DTG analysis data, therefore, further supports the use of 4.5 wt% biochar as the preferred formulation of the compositions tested.

Proposed flame-retardant mechanism

The flame-resistant properties of the flax/kenaf/sugarcane biochar hybrid composites are suggested to result from the combined contribution of the natural fibres and sugarcane biochar. The mechanism proposed is supported by the results of combined LOI, cone calorimeter, TGA/DTG and microstructural results that were obtained in this study. Thermal conductivity, oxygen permeability and gaseous combustion products were not measured directly and so the discussion given below is in the light of the possibility of the occurrence of each process rather than providing proof of each.

On exposure to external heat source, the epoxy matrix and lignocellulosic components decompose and release volatile products and solid carbonaceous char. Cellulose, hemicellulose and lignin are major components of the flax and kenaf fibres that will lead to a residue from the thermal decomposition. The sugarcane biochar contains an extra thermally stable carbon-rich phase in the composite. This effect is confirmed by the increase in char residue from 11% for neat epoxy (Sample A) to 28% in the 4.5 wt % biochar composite (Sample E). The residual char at 6 wt. % biochar was slightly reduced to 25%, suggesting that there is a slight decrease in the benefit of biochar beyond the optimum.

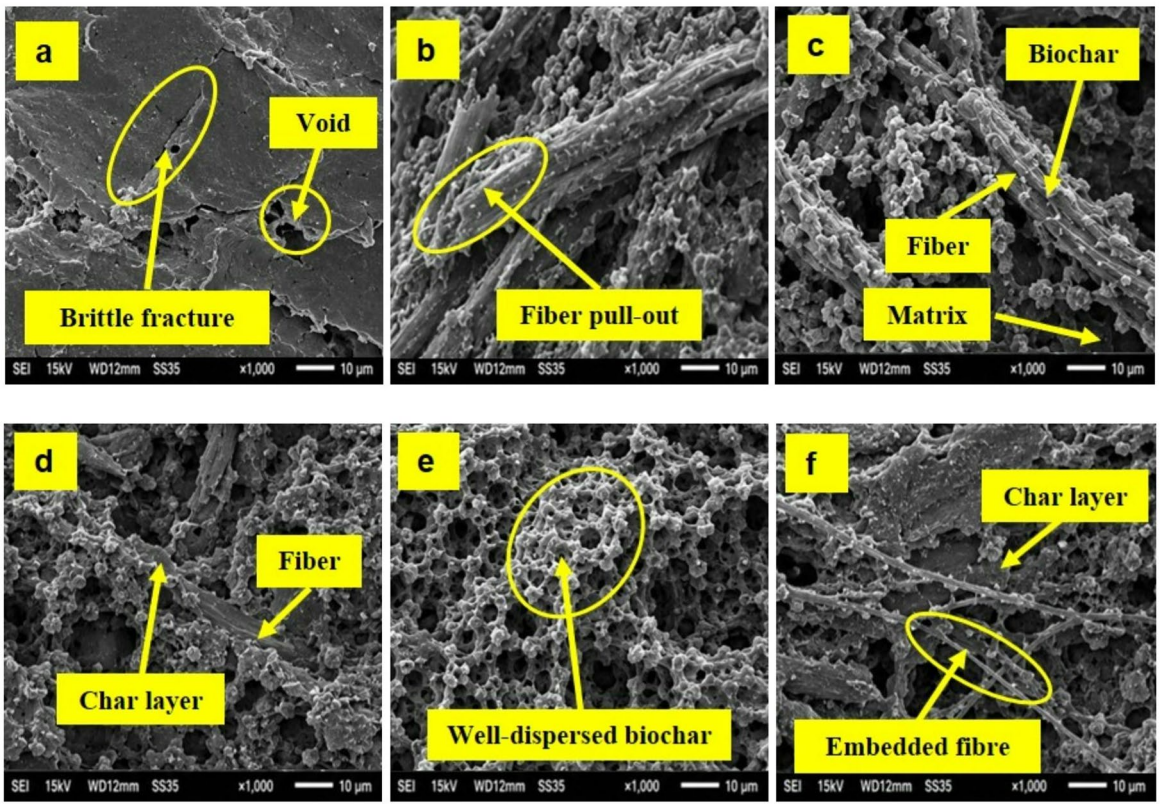


Fig. 29 SEM images of char residues after flammability testing of fabricated composites: (**a**) Sample A; (**b**) Sample B; (**c**) Sample C; (**d**) Sample D; (**e**) Sample E; and (**f**) Sample F.

The TGA data also show the thermal degradation resistance of the composite was enhanced with the addition of biochar. The onset degradation temperature increased from 278 °C for neat epoxy to 317 °C for Sample E with 4.5 wt% biochar. The DTG analysis showed T_{max} values of 393, 387, 385, 388, 394, and 390 °C for Samples A–F, respectively. The main DTG peak also decreased from −0.4630 to −0.4215 when the biochar content increased from 0 to 4.5 wt% for Samples A and E, respectively, showing that the maximum rate of mass loss at the optimum biochar content was lower for Sample E than for Sample A. There was a slight reversal in Sample F, at the DTG peak value of −0.4255. From these findings, the 4.5 wt% biochar composite has the most desirable properties of thermal degradation resistance and formation of char residue.

In combustion, the carbonaceous residue from the composite is suggested to deposit on the material surface as a condensed-phase protective layer. This could limit the amount of heat and oxygen that reaches the underlying polymer, and could hinder the release of volatiles from the polymer. Condensed phase protection has been reported for biochar in epoxy systems and also for systems based on agricultural wastes as a flame-retardant[25,45]. But the reduction in heat transfer or oxygen transport cannot be quantified in the present study since these properties were not measured directly.

The proposed mechanism is consistent with the measured fire performance results. At 4.5 wt% biochar, the LOI increased from 19.5±0.5% for Sample A to 28.4±0.8% for Sample E, while the PHRR decreased from 519.98±9.53 to 300.10±9.28 kW/m^2 and THR decreased from 78.02±1.72 to 54.03±1.74 MJ/m^2. The TTI increased from 32±2 to 61±2 s, and the burning rate decreased from 3.8±0.2 to 2.1±0.2 mm/min. The overall results suggest that the optimized biochar containing composite has a delayed ignition time, lower heat-release intensity, lower total heat release and slower burning rate.

This is supported morphologically by the SEM observations. The 4.5 wt% biochar composite (Sample E) had a relatively dense fracture structure, fewer visible voids, and better fibre encapsulation. This morphology is also



Fig. 30 Photographic image of the fabricated flax/kenaf/flax/sugarcane-biochar-based electrical conduit pipe.

consistent with the presence of a more integrated carbon-rich structure together with the higher residual char content. The 6 wt% biochar composites, on the other hand, exhibited more particle aggregation and discontinuities in the microstructure. This was accompanied by a reduction in T_{onset} from 317 °C to 313 °C and in residual char from 28 to 25%, together with a slight deterioration in the fire-performance parameters. The results indicated that applying excessive biochar loading and particle agglomeration may hinder the protective carbonaceous structure effect.

The overall result indicates that the flame-retardant properties of the bio-composite were correlated with the following: (i) higher amount of thermally stable carbonaceous residue, (ii) later onset of thermal degradation, (iii) lower maximum mass loss rates, and (iv) higher architecture density at optimal biochar loading. The carbon-rich residue is thus suggested to have a protective role in condensed phase during the combustion process[18,60]. The higher yield found with 4.5 wt% biochar followed by a decrease at 6 wt% suggests that there is an optimum amount of biochar for the range of formulations studied. Figure 27 depicts the suggested condensed-phase flame retardant mechanism, including the process of char formation facilitated by biochar and the modifications to key fire performance parameters and oxygen/volatile transport caused by it.

It is important to note that the present study did not measure thermal conductivity, oxygen permeability, smoke generation and CO / CO_2 emissions directly. As such the reduction in thermal conductivity, reduction in oxygen diffusion, smoke suppression or toxicity does not constitute an experimentally proven mechanism. To quantitatively confirm these individual mechanisms would require further investigation using thermal conductivity measurements, post combustion residue characterization, and combustion gas/smoke analysis.

Microstructural analysis

SEM analysis of tensile-fractured surfaces

The microstructural features of the fracture surfaces of the tensile-fractured samples of the developed flax/kenaf/flax/sugarcane-biochar hybrid composites were analyzed using scanning electron microscopy (SEM). The morphologies of the tensile fracture for the samples A–F are shown in Fig. 28. The fracture morphology, fibre–matrix interaction, visible voids and defects, fibre pull-out and effect of the biochar incorporation on the mechanical behavior of the developed composites were investigated by the SEM.

Figure 28 (a) shows the morphology of the neat epoxy specimen after tensile fracture, which is relatively smooth with fracture features resembling rivers, suggesting fracture behaviour to be comparatively brittle. The limited visible energy-dissipation features are consistent with the relatively lower mechanical properties of the neat epoxy sample, and the crack-propagation regions are visible. The flax/kenaf/flax hybrid composite without biochar (Fig. 28(b)) has a relatively coarse fracture surface, characterized by fibre pull-out and microvoids. These features suggest the contribution of the natural fibres to load transfer and energy dissipation during fracture. Similar relationships between matrix modification, interfacial characteristics and fracture resistance have been reported in fibre/epoxy composite systems[61]. But there is incomplete fibre–matrix contact as indicated around some fibre regions, which could have an effect on the mechanical response of the composite[62].

Table 7 Contextual comparison of selected reported characteristics of conventional PVC conduit materials and the developed flax/kenaf/flax epoxy composite containing 4.5 wt% sugarcane biochar for preliminary application assessment [68–70].

Property	Conventional PVC Conduit Pipe	Developed Flax/Kenaf/Flax + 4.5 wt% Sugarcane Biochar Composite Pipe	Data source / test condition
Base Material	Polyvinyl chloride (petroleum-derived thermoplastic polymer)	Epoxy matrix reinforced with flax/kenaf/flax fibres and sugarcane biochar	Material description
Density	Reported density depends on PVC grade and formulation	Not measured in the present study	PVC: formulation-dependent literature information; composite: not experimentally determined
Thermal Stability	Thermal behaviour depends on PVC formulation, stabilizers, and additives	TGA/DTG: T_{onset} = 317 °C; T_{max} = 394 °C; residual char = 28% for Sample E	Composite: measured by TGA/DTG
Flammability Behaviour	Fire behaviour depends on PVC grade, formulation, additives, and test conditions	Fire-performance parameters were experimentally determined using LOI, cone calorimetry, and horizontal burning tests	Composite: measured; test methods given in Section "Mechanical characterization"
Limiting Oxygen Index (LOI)	Reported values vary with PVC formulation and testing conditions; no PVC control was tested in the present study	28.4 ± 0.8% (Sample E)	Composite: ASTM D2863-17; n = 3
Peak Heat Release Rate (PHRR)	Reported values vary with PVC grade, formulation, specimen dimensions, and heat flux; no direct PVC comparison was performed	300.10 ± 9.28 kW/m^2 (Sample E)	Composite: ASTM E1354-17; external heat flux = 50 kW/m^2; n = 3
Total Heat Release (THR)	Depends on PVC formulation, specimen dimensions, and test conditions; no direct PVC comparison was performed	54.03 ± 1.74 MJ/m^2 (Sample E)	Composite: ASTM E1354-17; external heat flux = 50 kW/m^2; n = 3
Mechanical Performance	Established commercial use in conduit applications; performance depends on PVC grade and applicable standard	Tensile strength = 38.01 ± 0.55 MPa; Flexural strength = 76.12 ± 0.90 MPa; Impact strength = 9.62 ± 0.45 kJ/m^2 for Sample E	Composite: measured experimentally; ASTM methods described in Section "Thermal analysis (TGA/DTG)"
Fire Residue Behaviour	Depends on PVC composition and combustion conditions	Carbonaceous char residue observed after flammability testing; Sample E showed a relatively compact and continuous residue morphology	Composite: post-flammability SEM
Environmental Consideration	Petroleum-derived polymer system	Contains natural flax/kenaf fibres and sugarcane-waste-derived biochar	Material composition; no LCA performed
Application Status	Established commercial conduit material with applicable standards and certification requirements	Proof-of-concept cylindrical prototype; 300 mm length and 3 mm wall thickness	Composite: prototype fabricated in the present study
Electrical Performance	Commercial PVC conduit systems are subject to applicable electrical/conduit requirements	Not evaluated in the present study	Dielectric strength, insulation resistance, and volume resistivity require future evaluation
Required Validation Before Practical Use	Applicable standards/certification depend on conduit application	Further evaluation required, including dielectric strength, volume resistivity, insulation resistance, water absorption/moisture conditioning, compression, impact, bending, appropriate fire classification, IEC 61,386 conduit-specific testing, and long-term durability	Future validation [71]

The experimental values of composite were calculated in the present study. The numerical PVC values are not presented as direct comparators of conventional PVC control specimens because they were not tested under the same conditions. The PVC information is only given as an aid to context and reported performance will vary as a result of formulation, specimen geometry, additives and test conditions. In the present study, a life cycle assessment and a techno-economic analysis were not done.

When the 1.5 wt% biochar is added (Fig. 28 (c)), the fracture surface looks relatively more compact, and the biochar particles appear relatively well distributed in the matrix regions. The carbonaceous filler can play a role in enhancing the stress transfer in the epoxy matrix[63]. The incorporation of particulate fillers can modify the morphology and surface characteristics of polymeric systems, with particle size, morphology, surface area and matrix–filler interactions influencing the resulting material behaviour[64]. The fracture morphology at 3 wt% biochar (Fig. 28 (d)) shows a denser fracture morphology, along with less fibre pull-out, indicating better interaction between the reinforcement constituents and matrix[65]. The fracture surface for the 4.5 wt% biochar composite (Fig. 28 (e)) shows a relatively compact fracture surface, good fibre encapsulation and minimal visible interfacial defects. This morphology corresponds to the best tensile strength, flexural strength, impact strength and ILSS values recorded for Sample E. This superior mechanical performance could be related to more effective stress transfer between the flax/kenaf fibres, biochar and epoxy matrix.

The fracture surface at 6 wt% biochar (Fig. 28 (f)) shows more irregular areas and some defects, possibly due to a lower efficiency in dispersing the filler at the higher biochar concentration. However, higher biochar loading can create regions of high filler concentration and lower stress-transfer efficiency, which may be associated with early fracture initiation[66]. This observation agrees with the decrease in the mechanical properties measured for sample F as compared to sample E.

SEM analysis of char residues after flammability testing

The SEM analysis (Fig. 29) was also conducted on the char residue obtained from the flammability tests to gain insight into the flame-retardant mechanism of the hybrid composites. The char residue morphology gives insight into the carbonaceous structure that was developed during the combustion process and its possible protective barrier properties, whereas the tensile fracture surfaces do not.

The char morphology of Sample E with 4.5 wt% biochar (Fig. 29(e)) is the most compact and continuous among the samples, with good structural integrity and fewer visible cracks. This observation is consistent with the improved fire performance of Sample E, which exhibited the highest LOI value (28.4 ± 0.8%), lowest PHRR (300.10 ± 9.28 kW/m^2), and reduced THR (54.03 ± 1.74 MJ/m^2).

In the flax/kenaf hybrid composite without biochar (Fig. 29b), there is a fibrous carbonaceous residue resulting from the lignocellulosic reinforcement. Based on the observations, the fibre-derived char contributes to residue formation, but its structure is still not as compact as that developed by the biochar-containing composites. The biochar treatment (Samples C and D, Fig. 29 (c & d)) demonstrates increasing carbonaceous residue formation and more connected char structure with increasing amount of biochar. Biochar can encourage the formation of carbon-rich residue that can serve as a physical barrier and possibly help limit heat transfer and volatiles during combustion[25]. With 6 wt. % biochar loading (Fig. 29 (f)), carbonaceous residue is still present, but the carbonaceous residue is less uniform in its structure, with some visible defects. The reduced effectiveness of the protective char barrier may be associated with the slight decrease in LOI (26.7 ± 0.7%) and increase in PHRR (340.04 ± 9.37 kW/m^2) [67].

In general, the SEM observations reveal that the structure of char residue in the hybrid composites, as well as fracture morphologies, are affected by the incorporation of biochar. The observed carbonaceous char structure may contribute to the enhanced flame resistance, while the reinforcement interaction is associated with the mechanical performance.

Application of developed composite for electrical conduit pipe

The final flax/kenaf/flax composite formulation for the production of composite conduits was chosen from among the studied formulations based on the most favourable overall mechanical and fire-performance response (Sample E: 4.5 wt% sugarcane biochar). Sample E exhibited a tensile strength of 38.01 ± 0.55 MPa, flexural strength of 76.12 ± 0.90 MPa, impact strength of 9.62 ± 0.45 kJ/m^2, hardness of 86 ± 1 Shore D, and ILSS of

13.24 ± 0.35 MPa. In addition, the composite exhibited a LOI of 28.4 ± 0.8%, PHRR of 300.10 ± 9.28 kW/m^2, and THR of 54.03 ± 1.74 MJ/m^2, together with a TTI of 61 ± 2 s and a burning rate of 2.1 ± 0.2 mm/min. The findings in this study suggest that the composite developed could be further studied for its application in cases where a combination of mechanical functionality and enhanced fire performance features is desired. Photographic image of the fabricated electrical conduit pipe made of flax/kenaf/flax/sugarcane-biochar is shown in Fig. 30.

An electrical conduit pipe prototype was successfully produced from the developed composite material by a molding process. This pipe was made with a length of 300 mm and a wall thickness of 3 mm. The flax and kenaf fibre reinforcement helped to ensure the structural integrity of the fabricated pipe; the biochar added another carbonaceous phase in the epoxy matrix. The fabricated conduit had a good dimensional stability under the fabrication conditions of the present study and its intended tubular geometry was maintained.

The fire-performance criteria of the chosen composite are similar to those obtained for the thermal and flammability of Sample E. The TGA data and the results of LOI, ignition time, PHRR, THR and combustion rate indicates that the composite developed can be considered for use in applications where better resistance to combustion is required. These results do not, however, provide any indication of compliance with electrical-conduit fire-safety requirements, as they are for the material level.

The fabricated conduit pipe is a proof-of-concept demonstration of the application of natural fibres from agricultural wastes and sugarcane biochar to form a polymer composite structure. The present study is therefore demonstrating the feasibility to process the developed hybrid composite into a conduit-like geometry while maintaining the material characteristics of the mechanical, thermal and fire-performance evaluation[4].

PVC conduit materials have many properties that are well known from wide industrial use and provide good electrical insulation, mechanical strength and durability. Hence, it is not advisable to replace the conventional PVC conduit with the present composite, only on the basis of the results of this study. To make a meaningful comparison, identical testing conditions and evaluation of the electrical, mechanical, fire, smoke and durability properties would need to be applied to the comparable properties of the two products. Table 7 shows the comparison of some of the reported properties of PVC conduit materials and developed flax/kenaf/flax epoxy composite with 4.5 wt% of sugarcane biochar for preliminary assessment of application.

Other tests are needed for practical use of electrical conduit, such as electrical insulation characteristics (dielectric strength, volume resistivity, insulation resistance), and mechanical characteristics (impact resistance, compression resistance, dimensional stability and thermal stability), tests for environmental durability, and tests for standard fire performance for specific application. Further characterization of smoke and combustion gases would also be required before an enclosed electrical installation was determined to be suitable for use. In the present study UL-94 vertical burning classification was not determined, so there is no UL-94 rating for the developed composite. While sugarcane waste was the starting material for the biochar production, the present study did not estimate the energy required for each of the processes such as pyrolysis at 650 °C, cooling, ball milling, composite processing. Also, life-cycle assessment and techno-economic analysis were not done. Therefore, it is not possible to quantify the environmental and economic benefits of the developed composite from the present results. Energy accounting, life-cycle assessment and cost analysis of biochar production, composite fabrication, transportation, service life, and end-of-life management should be included in future studies. They are important shortcomings of the current research and should be considered in future research to define electrical-conduit application-specific performance, environmental impacts, economic feasibility, and practical suitability of the developed composite.

Overall, the fabricated conduit is a proof-of-concept demonstration showing that the flax/kenaf/flax hybrid composite made with sugarcane-biochar (4.5 wt%) can be successfully formed into the conduit-like structure. The mechanical, thermal stability, and fire-performance properties achieved for Sample E make it a suitable candidate for further application-specific development and testing.

Conclusion

This study proved that sugarcane biochar serves as an effective bio-derived filler to improve mechanical, thermal and fire performance properties of flax/kenaf/flax hybrid epoxy composites. The XRD, EDX and FTIR analysis confirmed the carbon rich and functional properties of sugarcane biochar and its integration in the hybrid composite system. Mechanical results showed a definite composition-dependent response – when biochar was added, mechanical properties increased till an optimum loading was reached and then decreased at 6 wt. % of biochar.

The 4.5 wt. % biochar (Sample E) formulation had the best overall mechanical performance, with a tensile strength of 38.01 ± 0.55 MPa, tensile modulus of 3.60 ± 0.20 GPa, flexural strength of 76.12 ± 0.90 MPa, flexural modulus of 4.80 ± 0.20 GPa, impact strength of 9.62 ± 0.45 kJ/m^2, hardness of 86 ± 1 Shore D and ILSS of 13.24 ± 0.35 MPa. The statistical analysis also showed that significant differences among the formulations investigated were present and the Tukey analysis showed that overall, the best performance was achieved by Sample E for most of the mechanical parameters investigated. The results of Sample D showed the highest elongation, indicating that the optimum formulation is dependent on the mechanical property.

The thermal and fire-performance results similarly confirmed that 4.5 wt% biochar is the best formulation in the range of values tested. Sample E had the highest T_{onset} (317 °C) and T_{max} (394 °C), the lowest principal DTG peak (−0.4215), and the highest residual char content (28%). Its fire-performance characteristics included an LOI of 28.4 ± 0.8%, PHRR of 300.10 ± 9.28 kW/m^2, THR of 54.03 ± 1.74 MJ/m^2, TTI of 61 ± 2 s, and burning rate of 2.1 ± 0.2 mm/min. The TGA/DTG and post-flammability SEM data supported the formation of more carbonaceous residue and a relatively compact char structure at this loading, consistent with the proposed condensed-phase flame-retardant mechanism.

The 4.5 wt% sugarcane-biochar-containing flax/kenaf/flax composite was successfully molded into a 300 mm long electrical conduit prototype with a 3 mm wall thickness, indicating the feasibility of producing the optimized material in the form of an electrical conduit prototype. Mechanical, thermal, and fire performance suggest that sugarcane biochar can provide multifunctional reinforcement to the natural-fibre/epoxy hybrid system. In conclusion, the study revealed that 4.5 wt% sugarcane biochar offered the best overall combination of mechanical and fire performance properties of the considered formulations, and the results of this study can serve as a basis for future research and development of bio-derived hybrid composite materials for use as fire-resistant materials in the manufacture of electrical conduits.

Supplementary Information The online version contains supplementary material available at https://doi.org/10.1038/s41598-026-80600-3.

Acknowledgements The authors gratefully thank the authors' respective institutions for their strong support of this study.

Author contributions Velmurugan Ganesan: Formal analysis, Investigation, Writing—original draft. Jasgurpreet Singh Chohan: Data curation, Formal analysis, Investigation, Writing—original draft. Muhammed Abraar S A: Conceptualization, Data curation, Formal analysis, Investigation, Writing—original draft. Velusamy K: Project administration, Writing – original draft, Writing – review and editing. Elil Raja D: Writing – original draft, Writing – review & editing. Ramya Maranan: Review and Editing. Arunprasath K: Review and Editing. Arun Kumar: Formal analysis, Investigation, Writing—original draft. Regasa Yadeta Sembeta: Writing – original draft, Writing – review and editing.

Funding No funding was received for this research work.

Data availability The article includes the data that was utilized to support the study's conclusions. If further data or information is needed, the appropriate author can provide it upon request.

Declarations

Competing interests The authors declare no competing interests.

Ethical approval Not applicable.

Consent to participate Not applicable.

Consent for publication Yes. All permission granted.

Open Access This article is licensed under a Creative Commons Attribution-NonCommercial-NoDerivatives 4.0 International License, which permits any non-commercial use, sharing, distribution and reproduction in any medium or format, as long as you give appropriate credit to the original author(s) and the source, provide a link to the Creative Commons licence, and indicate if you modified the licensed material. You do not have permission under this licence to share adapted material derived from this article or parts of it. The images or other third party material in this article are included in the article's Creative Commons licence, unless indicated otherwise in a credit line to the material. If material is not included in the article's Creative Commons licence and your intended use is not permitted by statutory regulation or exceeds the permitted use, you will need to obtain permission directly from the copyright holder. To view a copy of this licence, visit http://creativecommons.org/licenses/by-nc-nd/4.0/.

References

1. De, B., Bera, M., Bhattacharjee, D., Ray, B. C. & Mukherjee, S. A comprehensive review on fiber-reinforced polymer composites: Raw materials to applications, recycling, and waste management. *Prog. Mater. Sci.***146**, 101326 (2024).
2. Islam, T. et al. Advancements and challenges in natural fiber-reinforced hybrid composites: A comprehensive review. *SPE Polym.*https://doi.org/10.1002/pls2.10145 (2024).
3. Blythe, A., Fox, B., Nikzad, M., Eisenbart, B. & Chai, B. X. Stiffness degradation under cyclic loading using three-point bending of hybridised carbon/glass fibres with a polyamide 6, 6 nanofibre interlayer. *J. Compos. Sci.***6**, 270 (2022).
4. Mylsamy, B. et al. A review on natural fiber composites: Polymer matrices, fiber surface treatments, fabrication methods, properties, and applications. *Polym. Eng. Sci.*https://doi.org/10.1002/pen.26713 (2024).
5. Ulus, H., Manav, A. S. & Kaybal, H. B. Hygrothermal durability of Elium® glass–carbon hybrid laminates: Role of stacking architecture and data-driven sensitivity analysis. *Proc. Inst. Mech. Eng. L J. Mater. Des. Appl.*https://doi.org/10.1177/14644207261447288 (2026).
6. Mohammed, M. et al. A review on the advancement of renewable natural fiber hybrid composites: Prospects, challenges, and industrial applications. *J. Renew. Mater.*https://doi.org/10.32604/jrm.2024.051201 (2024).
7. Ramesh, M. Flax (*Linum usitatissimum* L.) fibre reinforced polymer composite materials: A review on preparation, properties and prospects. *Prog. Mater. Sci.***102**, 109–166 (2019).
8. Lei, L. et al. Improving the interfacial adhesion and mechanical properties of flax fiber reinforced composite through fiber modification and layered structure. *Ind. Crops Prod.***221**, 119305 (2024).
9. Malik, K. et al. Physical and mechanical properties of kenaf/flax hybrid composites. *J. Appl. Polym. Sci.***140**, e53421 (2023).
10. Hiremath, V. S., Reddy, D. M., Mutra, R. R., Sanjeev, A. & Dhilipkumar, T. Thermal degradation and fire retardant behaviour of natural fibre reinforced polymeric composites-A comprehensive review. *J. Mater. Res. Technol.***30**, 4053–4063 (2024).
11. Ao, X., Vázquez-López, A., Mocerino, D., González, C. & Wang, D.-Y. Flame retardancy and fire mechanical properties for natural fiber/polymer composite: A review. *Compos. Part B Eng.***268**, 111069 (2024).
12. Rajeshkumar, L., Kumar, P. S., Boonyasopon, P., Rangappa, S. M. & Siengchin, S. Flame retardance behaviour and degradation of plant-based natural fiber composites–a comprehensive review. *Constr. Build. Mater.***432**, 136552 (2024).
13. Muralidharan, N. D. et al. Flame retardant characteristics of natural fibre reinforced polymer composites: A thematic review. *Polym. Compos.***45**, 12530–12558 (2024).
14. Rex, P., Ganesan, V., Sivashankar, V. & Tajudeen, S. Prospective review for development of sustainable catalyst and absorbents from biomass and application on plastic waste pyrolysis. *Int. J. Environ. Sci. Technol.***20**, 8141–8156 (2023).
15. Das, O. et al. Functionalised biochar in biocomposites: The effect of fire retardants, bioplastics and processing methods. *Compos. Part C Open Access***11**, 100368 (2023).
16. Hoque, M. M. U., Bin, B. M. K., Chanda, A., Garcia-Perez, M. & Yadama, V. Engineering biochar–polymer interactions for sustainable composite applications: A review. *Biomass Bioenergy***217**, 109878 (2026).
17. Vivekanandhan, S. et al. A review of the unintended consequences of biochar in various applications. *Adv. Energy Sustain. Res.***7**, e202500505 (2026).
18. Tengku Yasim-Anuar, T. A. et al. Emerging application of biochar as a renewable and superior filler in polymer composites. *RSC Adv.***12**, 13938–13949 (2022).
19. Ren, J. et al. All-biomass derived nanocomposite films. *Nano Lett.***25**, 7810–7817 (2025).

20. Ren, J. et al. All-biomass nanocomposite films via facile and sustainable design procedure for thermal management and electromagnetic interference shielding. *Adv. Sci.***12**, e10372 (2025).
21. Yu, C. et al. Polypyrrole nanomorphology-driven sodium alginate based multifunctional hydrogels: Synergistic integration of mechanical robustness, electromagnetic shielding, and strain sensing. *Carbohydr. Polym.*https://doi.org/10.1016/j.carbpol.2026.125825 (2026).
22. Zuccarello, B. et al. New concept in bioderived composites: Biochar as toughening agent for improving performances and durability of agave-based epoxy biocomposites. *Polymers***13**, 198 (2021).
23. Lakshmana Kishore, T. & Erko, K. G. Mechanical properties of epoxy composite using papaya slice biochar and areca nut chopped fibre. *Adv. Polym. Technol.***2022**, 4733375 (2022).
24. Kumar, V., Arun, A., Rajkumar, K. & Palaniyappan, S. Effect of *Kigelia pinnata* biochar inclusion on mechanical and thermal properties of curtain climber fiber reinforced epoxide biocomposites. *Polym. Compos.*https://doi.org/10.1002/pc.28073 (2024).
25. Bifulco, A. et al. Coffee waste-derived biochar as a flame retardant for epoxy nanocomposites. *Sustain. Mater. Technol.***41**, e01079 (2024).
26. Sahoo, S. K. & Dash, B. P. Development and characterization of jute, coir and their hybrid composite materials with coconut shell biochar. *Next Res.***2**, 100595 (2025).
27. Rothenhäusler, F. et al. Influence of sodium hydroxide, silane, and siloxane treatments on the moisture sensitivity and mechanical properties of flax fiber composites. *Polym. Compos.***45**, 8937–8948 (2024).
28. Mani, S. K. et al. Advancements in chemical modifications using NaOH to explore the chemical, mechanical and thermal properties of natural fiber polymer composites (NFPC). *Int. Polym. Process.***39**, 406–432 (2024).
29. de Almeida, S. G. C., Tarelho, L. A. C., Hauschild, T., Costa, M. A. M. & Dussán, K. J. Biochar production from sugarcane biomass using slow pyrolysis: Characterization of the solid fraction. *Chem. Eng. Process. Process Intensif.***179**, 109054 (2022).
30. Varma, A. K. & Mondal, P. Pyrolysis of sugarcane bagasse in semi batch reactor: Effects of process parameters on product yields and characterization of products. *Ind. Crops Prod.***95**, 704–717 (2017).
31. Atmakuri, A., Palevicius, A., Janusas, G. & Eimontas, J. Investigation of hemp and flax fiber-reinforced EcoPoxy matrix biocomposites: Morphological, mechanical, and hydrophilic properties. *Polymers***14**, 4530 (2022).
32. Chai, B. X. et al. A novel heuristic optimisation framework for radial injection configuration for the resin transfer moulding process. *Compos. Part A Appl. Sci. Manuf.***165**, 107352 (2023).
33. de Oliveira, M. A., Souza, E. S., Correia, D. V., Barros, B. S. & Barros, J. K. Biochar derived from sugarcane bagasse for adsorption of anionic and cationic dyes. *Mater. Res.***28**, e20250179 (2025).
34. Zeng, X.-Y. et al. Impacts of temperatures and phosphoric-acid modification to the physicochemical properties of biochar for excellent sulfadiazine adsorption. *Biochar***4**, 14 (2022).
35. Kim, D.-Y. & Jung, G.-B. Effects of pyrolysis and ball-milling on the physicochemical and rhodamine B removal characteristics of rice-bran-derived biochar. *Appl. Sci.***13**, 4288 (2023).
36. Nzediegwu, C., Naeth, M. A. & Chang, S. X. Elemental composition of biochars is affected by methods used for its determination. *J. Anal. Appl. Pyrolysis***156**, 105174 (2021).
37. Ma, X.Z., Hao, X.Y., Chen, X.L., Gao, Z.C., Wei, D. and Zhou, B.K., Study on Biochar Properties Analysis with Scanning Electron Microscope-EnergyDispersive X-Ray Spectroscopy (SEM-EDX). Guang pu xue yu Guang pu fen xi= Guang pu 36:1670–1673 (2016).
38. Romanowska, B., Różańska, W. & Zimniewska, M. The influence of the chemical composition of flax and hemp fibers on the value of surface free energy. *Materials***17**, 1104 (2024).
39. Yu-Hao, D., Chun, C., Ping-Ping, W., Chun, W. & Xiong, F. Sugarcane extract enhances stress resilience and longevity in *Caenorhabditis elegans*: NMR structural elucidation and transcriptomic mechanisms. *Food Res. Int.*https://doi.org/10.1016/j.foodres.2025.117863 (2025).
40. Meraj, A. et al. Isolation and characterisation of lignin using natural deep eutectic solvents pretreated kenaf fibre biomass. *Sci. Rep.***14**, 8672 (2024).
41. Özgün, M. İ, Erci, V., Madenci, E. & Erci, F. The effect of nano-biochar derived from olive waste on the thermal and mechanical properties of epoxy composites. *Polymers***17**, 1337 (2025).
42. Somsole, L. N. et al. Experimental investigation and optimization of epoxy composites reinforced with jute fiber and alumina using the Jaya ANFIS approach. *Sci. Rep.***15**(1), 30462 (2025).
43. Alshahrani, H. & Prakash, V. R. A. Mechanical, fatigue and DMA behaviour of high content cellulosic corn husk fibre and orange peel biochar epoxy biocomposite: A greener material for cleaner production. *J. Clean. Prod.***374**, 133931 (2022).
44. Hidalgo, P., Salgado, L., Ibacache, N. & Hunter, R. Influence of biochar and bio-oil loading on the properties of epoxy resin composites. *Polymers*https://doi.org/10.3390/polym15081895 (2023).

45. Bartoli, M. et al. Influence of commercial biochar fillers on brittleness/ductility of epoxy resin composites. *Appl. Sci.***9**, 3109 (2019).
46. Aboughaly, M., Babaei-Ghazvini, A., Dhar, P., Patel, R. & Acharya, B. Enhancing the potential of polymer composites using biochar as a filler: A review. *Polymers***15**, 3981 (2023).
47. Matykiewicz, D. Biochar as an effective filler of carbon fiber reinforced bio-epoxy composites. *Processes***8**, 724 (2020).
48. Ap, A., Kaliappan, S. & Patil, P. Mechanical, fracture toughness, and dynamic mechanical properties of twill weaved bamboo fiber-reinforced *Artocarpusheterophyllus* seed husk biochar epoxy composite. *Polym. Compos.***43**, 8388–8395 (2022).
49. Ulus, H. et al. Functionally graded nanofiber interlayers for hydrothermally aged glass/epoxy laminates: Mechanical performance and electromagnetic attenuation. *Polym. Compos.*https://doi.org/10.1002/pc.71448 (2026).
50. Anbuchezhiyan, G. et al. Punch-shear behaviour of biochar-modified jute fibre-reinforced epoxy composites under different indenter geometries. *Polym. Test.*https://doi.org/10.1016/j.polymertesting.2026.109333 (2026).
51. da Cunha, J. D. et al. Physical and mechanical characterization of titica vine (Heteropsis flexuosa) incorporated epoxy matrix composites. *Polymers***13**, 4079 (2021).
52. Bachtiar, E. V., Kurkowiak, K., Yan, L., Kasal, B. & Kolb, T. Thermal stability, fire performance, and mechanical properties of natural fibre fabric-reinforced polymer composites with different fire retardants. *Polymers***11**, 699 (2019).
53. Das, O., Sarmah, A. K. & Bhattacharyya, D. A sustainable and resilient approach through biochar addition in wood polymer composites. *Sci. Total Environ.***512**, 326–336 (2015).
54. Shah, AurR. et al. Mechanical, thermal, and fire retardant properties of rice husk biochar reinforced recycled high-density polyethylene composite material. *Polymers***15**, 1827 (2023).
55. Mazzuoccolo, I. et al. Self-extinguishing and hydrophobic epoxy composites containing hydrothermal liquefaction-derived biochar and whisker-like particles based on tailored PVP-coated silica fibers. *Sustain. Mater. Technol.***47**, e01900 (2026).
56. Cong, X. et al. Investigation of fire protection performance and mechanical properties of thin-ply bio-epoxy composites. *Polymers***13**, 731 (2021).
57. Ghosh, S. K., Misra, M., Kiziltas, A., Prevoir, S. & Mohanty, A. K. Recent progress in flame retardancy of graphene and bio-based sustainable flame retardants for polymer composite applications. *Compos. Part C: Open Access*https://doi.org/10.1016/j.jcomc.2025.100637 (2025).
58. Hadou, A., Belaadi, A., Boumaaza, M., Abdullah, M.M., Ghernaout, D., Bourmaud, A. and Mukalazi, H. Thermomechanical properties of bio-based epoxy biocomposites reinforced with Dracaena draco fibrils and biochar: performance optimization using artificial neural networks. *Sci. Rep.* (2026).
59. Minugu, O. P., Gujjala, R., Shakuntala, O., Manoj, P. & Chowdary, M. S. Effect of biomass derived biochar materials on mechanical properties of biochar epoxy composites. *Proc. Inst. Mech. Eng. C J. Mech. Eng. Sci.***235**, 5626–5638. https://doi.org/10.1177/0954406221990705 (2021).
60. Taib, M. N. A. M. et al. Current progress of biopolymer-based flame retardant. *Polym. Degrad. Stabil.***205**, 110153 (2022).
61. Beylergil, B., Ulus, H., Al-Nadhari, A. & Yildiz, M. Enhanced fracture toughness and controlled curing of basalt fiber/epoxy composites via PPE powder modification. *Eng. Fract. Mech.*https://doi.org/10.1016/j.engfracmech.2026.112208 (2026).
62. Zheng, K. & Huang, C. Research on the interfacial reinforcement mechanism and tribological performance of resin matrix composites reinforced with alumina sol-modified coconut shell fibers. *Tribol. Int.*https://doi.org/10.1016/j.triboint.2026.112580 (2026).
63. Çetin, M. E., Üstün, A., Erdal, M. O. & Ulus, H. Recycled polyacrylonitrile nanofiber interleaves with graphene nanoplatelets for adhesively bonded composite joints: Lap-shear and opening-mode fracture performance. *Polym. Compos.*https://doi.org/10.1002/pc.71342 (2026).
64. Shankar, V. S. et al. A review on the development of silicon and silica based nano materials in the food industry. *SILICON***16**, 979–988 (2024).
65. Rajendran, S. et al. Enhancing carbon fiber composites with fish scale biochar for superior strength and environmental sustainability. *Clean. Eng. Technol.***27**, 100996 (2025).
66. Palaniappan, M., Kumar, P. M., Sivanantham, G. & Gebreyohannes, D. T. Chemical and structural characterization of ramie-based epoxy composites reinforced with macadamia nut shell biochar. *Sci. Rep.***16**, 9374 (2026).
67. Gaidhani, A., Jayaraman, H. V., Edwards, S., Tribe, L. & Charpentier, P. Mechanically robust biochar-modified polystyrene foam with enhanced flame retardancy using halogen-free additives. *Polym. Int.*https://doi.org/10.1002/pi.70155 (2026).
68. Ekelund, M., Edin, H. & Gedde, U. W. Long-term performance of poly (vinyl chloride) cables. Part 1: Mechanical and electrical performances. *Polym. Degrad. Stabil.***92**, 617–629 (2007).
69. Hirschler, M. M. Poly (vinyl chloride) and its fire properties. *Fire Mater.***41**, 993–1006 (2017).
70. Esmail, A. Impact of PVC mixtures of the electrical conduit on the physical properties. *FES J. Eng. Sci.***10**, 20–27 (2021).
71. Arunprasath, K. et al. Comprehensive review of advances in natural fiber composites for conductive and EMI shielding applications: Materials, mechanisms, and future prospects. *Int. J. Biol. Macromol.***320**, 145892 (2025).

Publisher's note Springer Nature remains neutral with regard to jurisdictional claims in published maps and institutional affiliations.

Authors and Affiliations

G. Velmurugan[1] · Jasgurpreet Singh Chohan[2] · S. A. Muhammed Abraar[3] · K. Velusamy[4] · D. Elil Raja[5] · Ramya Maranan[6] · K. Arunprasath[1] · Arun Kumar[7] · Regasa Yadeta Sembeta[8]

✉ Regasa Yadeta Sembeta
yadetaregasa@gmail.com

1 Department of Mechanical Engineering, Vel Tech Rangarajan Dr. Sagunthala R&D Institute of Science and Technology, Chennai 600 062, India

2 Department of Mechanical Engineering, University Centre for Research and Development, Chandigarh University, Gharuan Mohali 140 413, India

3 Department of Mechanical Engineering, St. Joseph's Institute of Technology, OMR, Chennai 600 119, India

4 Department of Mechanical Engineering, Annai Mathammal Sheela Engineering College, Erumapatty, Namakkal 637 013, India

5 Department of Mechanical Engineering, Saveetha Engineering College, Thandalam, Chennai 602 105, India

6 Division of Research and Development, Lovely Professional University, Jalandhar - Delhi G.T.Road, Phagwara 144 411, India

7 Center of Promotional Research, Graphic Era (Deemed to Be University), Dehradun, India

8 Department of Civil Engineering, College of Engineering and Technology, Mattu University, 318 Metu, Ethiopia